Cellular and Molecular Neurobiology (2025) 45:27
https://doi.org/10.1007/s10571-025-01547-z

ORIGINAL RESEARCH

Investigating Molecular Mechanisms in Ischemic Preconditioning-Induced Resiliency to Severe Acute Global Cerebral Ischemia Using a Mouse Model of Chronic Cerebral Hypoperfusion

Roli Kushwaha[1,3] · Shashikant Patel[1,3] · K. S. Yuvaraj[1] · Pooja Sharma[1] · Arvind Kumar[2,3] · Sumana Chakravarty[1,3]

Received: 10 January 2025 / Accepted: 17 March 2025
© The Author(s) 2025

Abstract
Cerebral ischemic preconditioning offers a promising strategy to enhance resilience to severe ischemic insults. Unilateral common carotid artery occlusion (UCCAo) is a valuable model to simulate chronic cerebral hypoperfusion (CCH). This study explored UCCAo-induced CCH as a preconditioning stimulus to induce ischemic tolerance against transient global cerebral ischemia (tGCI) induced by bilateral common carotid artery occlusion (BCCAo) in both male and female mice. We evaluated the effects of CCH preconditioning on neuroprotection and recovery through behavioral, histopathological, and molecular analyses. Laser Doppler Imaging (LDI) confirmed significant cerebral hypoperfusion post-UCCAo. Preconditioning reduced mortality rates at days 1 and 7 post-surgery as compared to BCCAo, suggesting its neuroprotective potential. Neurodeficit scoring demonstrated significant protection in preconditioned animals with recovery aligning closer to sham controls. Behavioral assays revealed improved motor and cognitive outcomes in preconditioned groups, with sex-specific differences evident in recovery dynamics. Molecular analyses indicated reduced reactive astrocyte (GFAP) and microglial (IBA1) activation in preconditioned animals, reflecting controlled glial responses. Sex-dependent variations in markers of hypoxia (*Hif1a*), autophagy (*Becn1*), and neurogenesis (S*ox2*) highlighted neuroadaptive and cellular influences on ischemic resilience. Preconditioning enhanced synaptic plasticity by upregulating PSD-95, synaptophysin and BDNF levels. In addition, preconditioning increased VEGF expression in blood serum reflecting vascular remodeling and neuroprotective angiogenesis. This study positions UCCAo-induced CCH as a reliable model for exploring ischemic tolerance mechanisms to advance therapeutic strategies for mitigating the effects of ischemic stroke.

✉ Sumana Chakravarty
sumanachak@iict.res.in; sumana98@gmail.com

[1] Department of Applied Biology, CSIR-Indian Institute of Chemical Technology (IICT), Tarnaka, Hyderabad, Telangana 500007, India

[2] CSIR-Centre for Cellular and Molecular Biology, Hyderabad, India

[3] Academy of Scientific and Innovative Research (AcSIR), Ghaziabad, UP 201002, India

Published online: 26 March 2025

Graphical Abstract

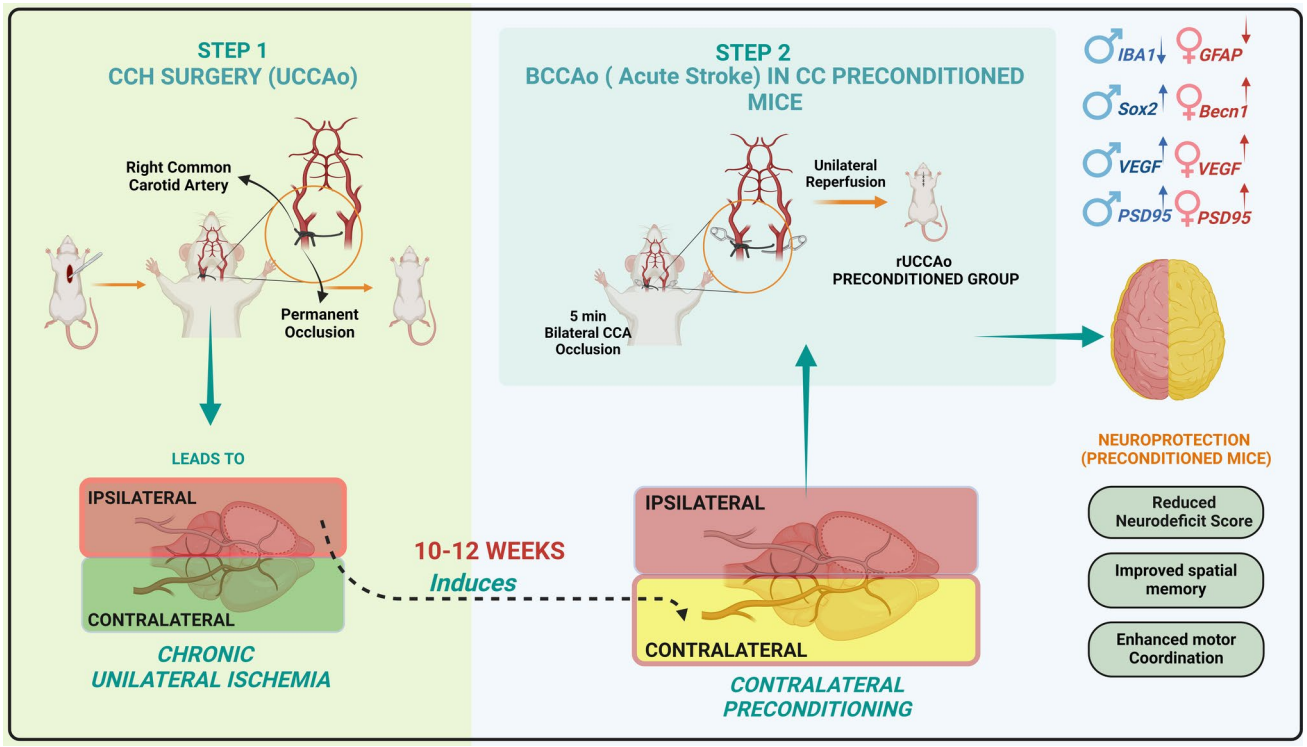

Keywords Neuroprotection · Chronic ischemia · Astroglial activation · Striatum · Cognitive impairments · Sex differences

Abbreviations

CCH	Chronic Cerebral Hypoperfusion
GST	Grip Strength Test
BBB	Blood–Brain Barrier
NVC	Neurovascular Coupling
IPC	Ischemic Preconditioning
CMH	Chronic Mild Hypoperfusion
BCCAo	Bilateral Common Carotid Artery Occlusion
MCAo	Middle Cerebral Artery Occlusion
UCCAo	Unilateral Common Carotid Artery Occlusion
RIC	Remote Ischemic Preconditioning
rUCCAo	Right Unilateral Common Carotid Artery Occlusion
lCCA	Left Common Carotid Artery
rCCA	Right Common Carotid Artery
OFT	Open Field Test
NORT	Novel Object Recognition Test
LDI	Laser Doppler Imaging
NDS	Neurological Deficit Score
GFAP	Glial Fibrillary Acidic Protein
IBA1	Ionized Calcium-Binding Adapter Molecule 1

Introduction

Chronic cerebral hypoperfusion (CCH) is a condition associated with persistent reduction in cerebral blood flow leading to vascular cognitive impairment and neurodegeneration (Wang et al. 2016). While ischemic stroke represents an acute and focal disruption in blood flow, CCH represents a more insidious and global reduction in perfusion that contributes to gradual neuronal dysfunction (Jing et al. 2015). Both conditions share overlapping pathophysiological mechanisms including blood–brain barrier (BBB) disruption, impaired neurovascular coupling (NVC), and secondary neuroinflammation. Recent studies have increasingly focused on investigating the ischemic preconditioning mechanisms, particularly using mice and other animal models (Das et al. 2020; Brancaccio et al. 2022). CCH, before a severe ischemic attack, can act as a form of preconditioning and can stimulate compensatory mechanisms such as enhanced collateral circulation (alternative blood flow pathways) and neuronal resilience through distinct molecular pathways. Contrary to this CCH, following an ischemic stroke exacerbates brain injury by further compromising cerebral blood flow leading to increased ischemic damage, brain edema, and neuroinflammation (Bin et al. 2017). This

compounded ischemic burden impairs the brain's ability to recover, worsens tissue integrity, and increases the risk of reperfusion hemorrhages. In addition, CCH leads to BBB disruption, impeding the clearance of neurotoxic proteins and, thus, contributing to long-term cognitive deficits, post-stroke dementia (Du et al. 2024), and post-stroke depression (Patel et al. 2024; Varghese et al. 2024).

Ischemic preconditioning (IPC) refers to the phenomenon wherein brief sublethal ischemic events render tissues more resistance to subsequent ischemic injuries (Murry et al. 1986). Molecular adaptations preserve cellular homeostasis, suppress apoptotic cascades, and mitigate ischemic damage. Global ischemia models like the four-vessel occlusion (4Vo) and bilateral common carotid artery occlusion (BCCAo) have highlighted region-specific vulnerabilities particularly in the striatum and hippocampus providing insights into neurovascular interactions, BBB integrity, and cognitive deficits (Wahul et al. 2018; Ojo et al. 2023). In contrast, the middle cerebral artery occlusion (MCAo) model which mimics human ischemic stroke by targeting the middle cerebral artery allows for precise investigation of localized ischemic damage and has also been utilized for understanding IPC as a protective strategy at multiple instances (Bowen et al. 2006; Yang et al. 2020).

The unilateral common carotid artery occlusion (UCCAo) model has traditionally been employed to simulate CCH and vascular dementia (VaD; Zhao and Gong 2015; Kim et al. 2023). However, its application as a preconditioning stimulus to induce ischemic tolerance has not been explored. Unlike remote ischemic preconditioning (RIC) which involves ischemic stimuli to distant organs, the UCCAo model directly affects cerebral circulation avoiding the systemic effects seen in remote models. This localized approach provides an opportunity to study brain-specific mechanisms of resilience and protection in response to ischemic stress. In the current study, we have developed a novel application of the UCCAo model as a preconditioning stimulus and investigated its potential to induce ischemic tolerance against severe ischemic insult by BCCAo. While CCH is associated with detrimental effects, we aimed to leverage CCH as a model to investigate the mechanistic pathways underlying ischemic resiliency mechanisms.

Emerging evidence highlights the critical role of sex as a biological variable in ischemic brain injury and recovery, with differences in vascular architecture, hormonal influences, and molecular mechanisms contributing to sex-specific outcomes (Tang et al. 2022). The preconditioning strategy was designed to induce ischemia on one side of the brain, thereby preconditioning the contralateral hemisphere to adapt and mitigate the effects of subsequent global ischemia. We hypothesized that unilateral IPC through permanent right common carotid artery occlusion (rUCCAo) could enhance the brain's resilience in both male and female mice by activating protective molecular and cellular mechanisms in the contralateral hemisphere. However, we also anticipated that sex-specific differences in these molecular and cellular responses might influence the extent of ischemic resilience during a subsequent BCCAo-induced severe ischemic insult.

We assessed both locomotor and cognitive outcomes which are critically impacted in ischemic events and essential for evaluating functional recovery. We performed behavioral studies to evaluate both early and delayed responses on days 1 and 7 post-surgery (refer to the experimental strategy). In addition, molecular analyses were focused on elucidating the early effects of BCCAo and preconditioning on the contralateral striatum owing to known effects of acute ischemia in this region (Wahul et al. 2018; Radhakrishnan et al. 2024a). Results indicated improved motor and cognitive recovery in preconditioned mice compared to the BCCAo group suggesting the neuroprotective potential of preconditioning.

Materials and Methods

Experimental Strategy

Adult CD1 male and female mice aged 22–25 weeks were used for all experiments. Upon procurement, the mice were acclimated to the housing facility. Following habituation, baseline behavioral testing was conducted using the open field test (OFT) at day 7 and the novel object recognition test (NORT) at day 10. These tests assessed the motor coordination and cognitive abilities of the animals. Mice that exhibited behavioral impairments were excluded from further experimentation. Healthy mice were segregated into three experimental groups; sham, preconditioning (PC), and BCCAo for both male and female experimental cohorts. For this study, a total of 150 mice were initially procured, with separate cohorts for males and females. Experiments were pre-designed to ensure that, even after accounting for animals excluded based on baseline behaviors and mortality in the BCCAo and PC groups post surgeries, each experimental group retained at least 9–12 mice. The preconditioning and surgical strategies employed in the study are illustrated in Fig. 1 while Fig. 2 outlines the sequence and timeline of the experiments.

On day 15, surgical interventions were carried out only for the PC group, where the right unilateral common carotid artery was permanently occluded (rUCCAo) to induce CCH. After 10–12 weeks interval, these same mice underwent further surgical intervention (referred to as post-stroke day 0 in Fig. 2) to induce bilateral ischemia, mimicking BCCAo-induced acute ischemic insult. This 10–12-week interval was selected to ensure the development of CCH post-rUCCAo

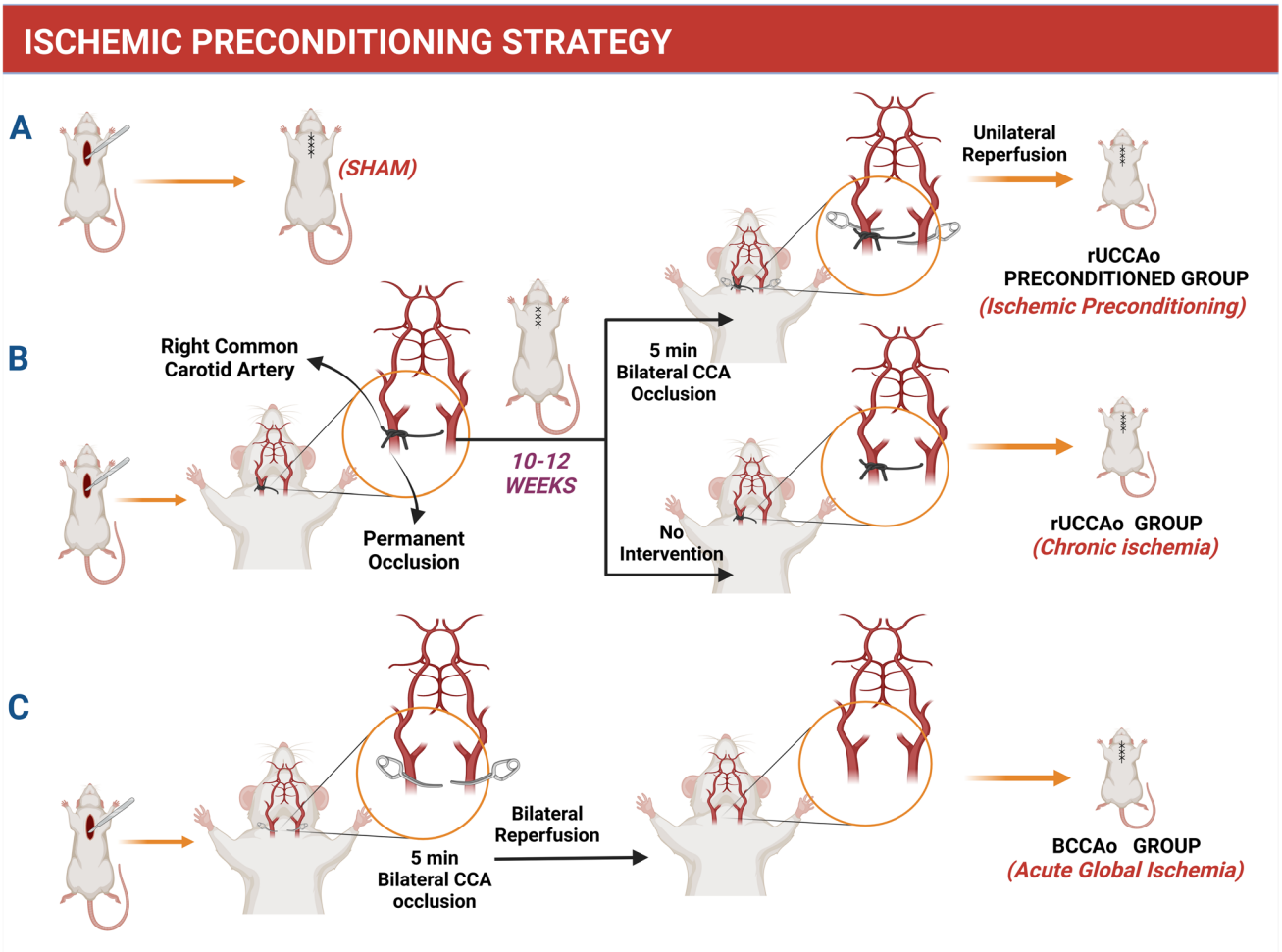

Fig. 1 Schematic representation of ischemic preconditioning and surgical strategies. **A** Sham surgery: a midline incision was made at the neck without any occlusion of the common carotid arteries. **B** Preconditioning surgery: permanent occlusion of the right common carotid artery (rCCA), followed by a subsequent surgical intervention after 10–12 weeks; where bilateral common carotid arteries (CCAs) were occluded for 5 min. In this procedure, the left common carotid artery (lCCA) was reperfused while the rCCA remained permanently occluded. **C** BCCAo (bilateral common carotid artery occlusion) surgery: bilateral occlusion of both common carotid arteries for 5 min, followed by bilateral reperfusion

and the establishment of CCH-mediated ischemic preconditioning effects, as these are time-dependent processes. During this procedure, both common carotid arteries were occluded for 5 min to induce transient global ischemia followed by unilateral reperfusion of the left common carotid artery (lCCA). Note that the rCCA which had been previously permanently occluded remained in this state throughout. Proximately respective surgeries were done in sham and BCCAo group as well. In the sham group, a midline incision was made at the neck under anesthesia, but no arteries were occluded. In the BCCAo group, both common carotid arteries were occluded simultaneously for 5 min followed by bilateral reperfusion of the arteries. Post-surgical assessments were conducted to evaluate immediate and delayed effects of ischemia and reperfusion at post-stroke days 1 and 7 (note that days 1 and 7 further on refer to days post-surgical interventions in sham, BCCAo and PC groups). While behavioral assessments were conducted at both days 1 and 7 to evaluate functional recovery over time, in this study for molecular analyses, we focused on day 1 post-surgery to understand the immediate effects of preconditioning which is critical for understanding the early molecular mechanisms underlying ischemic resilience. Contralateral striatal tissue samples were collected from these animals to perform molecular and histological analyses.

Behavioral Tests

Day 1 evaluations included the grip strength test (GST), rotarod test and neurological-deficit score (NDS). Day 7 assessments comprised the Y-maze test, rotarod test, OFT, NORT, GST, and NDS. These timings of behavioral

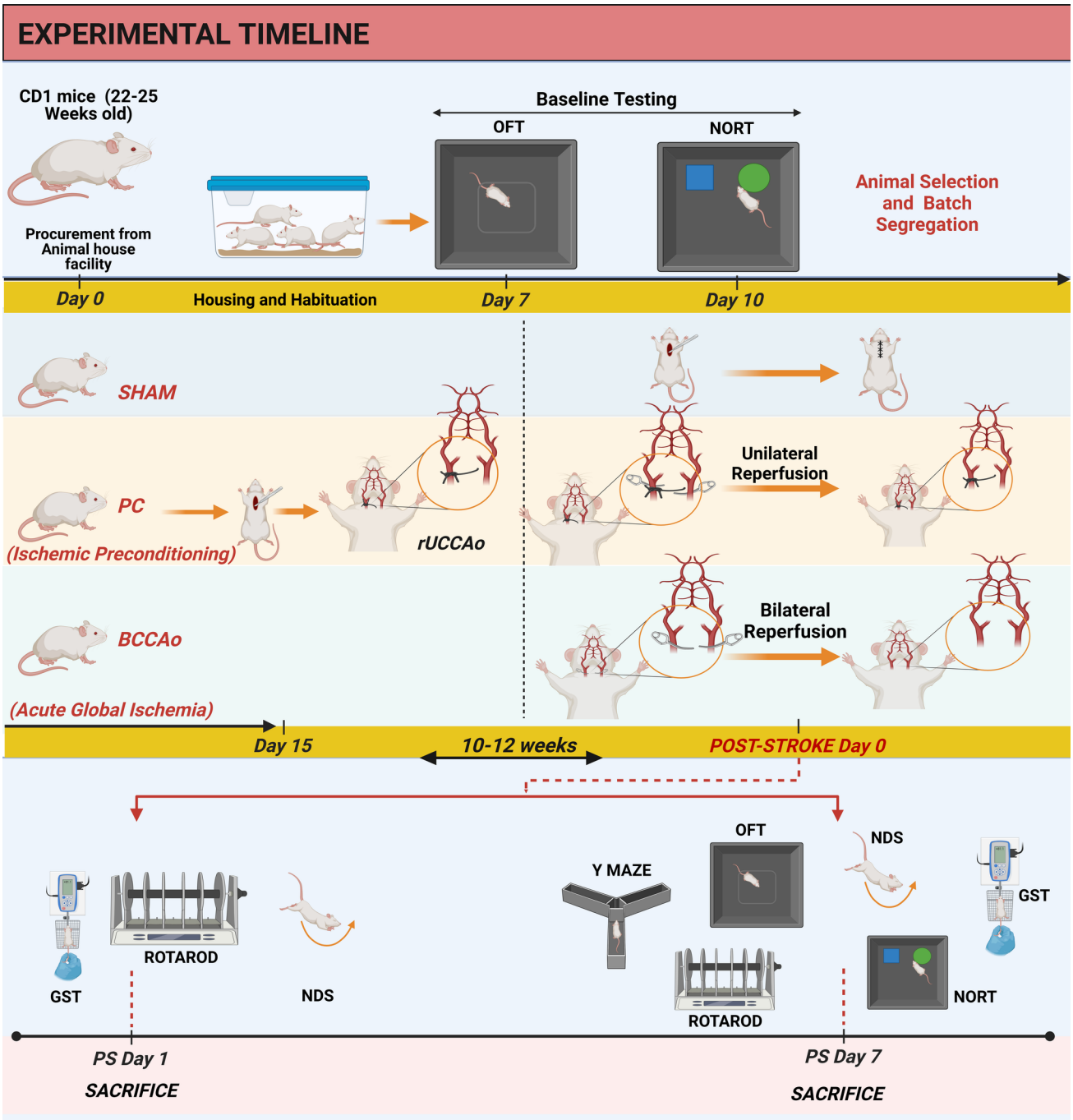

Fig. 2 Experimental timeline**.** This figure depicts the sequential stages of the study conducted on both male and female CD1 mice. Mice were procured and acclimatized in the animal facility for 7 days. Baseline behavioral tests included the Open Field Test (OFT) and Novel Object Recognition Test (NORT) to evaluate motor coordination and cognitive performance. Based on baseline results, mice with impairments were excluded and the remaining mice were segregated into sham, preconditioning (PC), and bilateral common carotid artery occlusion (BCCAo) groups. On day 15, preconditioning surgery involving permanent right common carotid artery (rCCA) occlusion was performed in the PC group. After 10–12 weeks, PC group mice underwent bilateral common carotid artery (CCA) occlusion. Simultaneously, the Sham and BCCAo groups underwent their respective surgeries as mentioned in Fig. 1. Behavioral assessments were conducted on days 1 and 7 post-surgery

tests were carefully designed to account for both acute and delayed effects of stroke. Day 1 evaluations were conducted to capture immediate deficits while these tests were repeated on day 7 to evaluate recovery and the long-term efficacy of preconditioning. Cognitive tests (NORT, Y-Maze) were conducted only on day 7 to avoid

confounding by acute motor impairments, such as reduced mobility, which could lead to inaccurate interpretation of cognitive performance. Additionally, cognitive deficits following stroke are a delayed consequence, making day 7 a more appropriate timepoint to assess these effects and the protective role of preconditioning.

Neurological-Deficit Score (NDS)

Neurological-deficit scoring was performed to assess the extent of impairment following surgical interventions using standard procedures (Wahul et al. 2018). The scoring was based on the presence and severity of specific behavioral symptoms. Briefly, a score of 0 was assigned when no symptoms or impairments were observed. If ptosis was noted in one or both eyelids a score of 1 was given. A score of 1.5 was assigned when body bending was observed and a score of 2 was given if both forelimb tremors and body bending were present. A score of 2.5 was assigned for weak locomotion, and a score of 3 was given if all the symptoms were simultaneously observed.

Rotarod Test

Prior to the surgical intervention animals (post-baseline assessment) underwent rotarod (UgoBasile, Italy) training for 3–4 consecutive days. During the training session, animals were trained to maintain balance for at least 180 s during 300 s assessment. To ensure retention of motor coordination, animals were re-assessed on the rotarod apparatus the day before surgical procedures confirming that the training effect persisted. Following the surgical intervention, rotarod testing was performed on days 1 and 7 post-surgery. The primary outcome measure was the latency to fall which provided a quantitative evaluation of motor coordination.

Grip Strength Test (GST)

The Grip Strength Test (GST) was used to assess forelimb strength in rodents. This test was performed on days 1 and 7 post-surgical intervention using a grip strength meter (Ugo Basile, Italy) following established protocols. Briefly each animal was placed in an inclined position on a mesh connected to a transducer. A gentle pulling force was applied to detach the animal from the mesh and the force exerted by the animal to resist this pull was measured in Newton (N). Grip strength was assessed through three separate measurements, and the average of these measurements was calculated to determine the forelimb strength.

Open Field Test (OFT)

To evaluate locomotor activity, OFT was conducted at baseline and on post-stroke day 7 to evaluate changes in motor activity over time. The test was performed in a rectangular wooden arena measuring 40 × 40 × 30 cm. Prior to the test, mice were acclimated to the testing room for 30–45 min to minimize environmental stress. Each mouse was allowed a 5-min period of free exploration in the arena during which locomotor activity parameters such as mean velocity and total distance traveled was recorded.

Novel Object Recognition Test (NORT)

Following surgery, animals in the sham, BCCAo, and PC groups underwent novel object recognition (NOR) training on day 6 in a 40 × 40 × 30 cm square box. During the training, two identical familiar objects were placed in the arena and the animals were allowed to explore for 10 min. On day 7, the animals were tested in the same arena where one of the familiar objects was replaced with a novel object differing in shape and color. The animals were given 5 min to explore both objects. Discriminative index (DI) was calculated using the formula:

$$\mathrm{DI} = \frac{\text{Time spent exploring the novel object}}{\text{Total time spent exploring both objects}}.$$

Y-Maze Test

In the Y-maze behavioral test, two different types of tests were performed to assess spatial memory and spatial working memory. Novel arm maze test was used to assess spatial memory. Mice were trained on day 6 post-surgery by placing them in the Y-maze where one arm was closed and they were allowed to explore for 10 min. After 24 h on day 7, the mice were reintroduced to the maze for 5 min where all arms were open. The duration and frequency of the mice's exploration in the novel arm were recorded to assess their spatial memory. Further spontaneous alternation was used to assess spatial working memory. For this test, mice were placed in one of the arms of the Y-maze and allowed to explore for 8 min. The spontaneous alternation score was calculated as the percentage of alternating entries between the arms using the formula:

$$\text{Spontaneous Alternation (\%)} = \left(\frac{\text{Number of spontaneous alternations}}{\text{Total number of arm entries} - 2}\right) \times 100.$$

Laser Doppler Imaging (LDI)

To assess blood perfusion rates during CCH, we employed laser Doppler imaging (LDI) using the Moor LDI2-HR Laser Doppler Imager (Moor Instruments, UK). The aim of this procedure was to evaluate the effects of UCCAo on blood perfusion, specifically assessing the decrease in perfusion post-occlusion. LDI was performed at three key time points: before occlusion, 1 h after occlusion and 14–16 weeks post-occlusion.

Immunofluorescence

Immunofluorescence (IF) was performed on 30 µm coronal brain sections from the striatum. After intracardiac perfusion with 4% paraformaldehyde (PFA) and post-fixation, brains were dehydrated in 30% sucrose. Sections were mounted on glass slides, permeabilized, and blocked with a solution containing 1% BSA and 4% NHS. Sections were incubated overnight with primary antibodies targeting IBA1 (Ionized Calcium-Binding Adapter Molecule 1) and GFAP (Glial Fibrillary Acidic Protein) followed by secondary antibody incubation and DAPI counterstaining. Confocal images were captured using an FV10i confocal laser Scanning microscope (Olympus, Japan), and expression analysis was performed using ImageJ software. Details of antibodies are provided in Supplementary Table 2.

RNA Isolation and Gene Expression Studies

Total RNA was extracted from the striatal tissue using TRIzol Reagent (Invitrogen, USA) according to the manufacturer's instructions. The extracted RNA was then used to synthesize cDNA utilizing the ThermoFisher first-strand cDNA synthesis kit following the standard protocol provided by the manufacturer. Quantitative real-time PCR (qPCR) was performed in triplicates with the SYBR Green PCR master mix detection system (Bio-Rad CFX 96). *Rpl32* was used as the housekeeping gene. Relative gene expression analysis was performed for *Hif1a* (Hypoxia-Inducible Factor 1-alpha), *Becn1* (Beclin 1), *Il1b* (Interleukin-1 beta), *Sox2* [SRY (Sex Determining Region Y)-Box 2], and *Il6* (Interleukin-6). Data analysis was conducted using the $\Delta\Delta C_t$ method to calculate relative expression levels. Primer sequences used in this study are detailed in Supplementary Table 1.

Immunoblotting

Proteins were isolated from the pink layer obtained during Trizol-based RNA extraction from striatal tissues. The protein pellet was dissolved in urea buffer and incubated overnight at 4 °C. The dissolved proteins were vortexed, centrifuged, and sonicated for further analysis. Protein concentrations were determined using Bradford assay. For protein separation, 30 µg of protein from each sample was loaded into SDS-PAGE gels and transferred onto PVDF membranes. The membranes were incubated with primary antibodies specific to BDNF, PSD-95, and SYN and normalized using α-tubulin as the loading control. After washing, blots were incubated with HRP-conjugated secondary antibodies for detection. Densitometric analysis was performed using ImageJ software. The details of antibodies used are listed in Supplementary Table 2.

ELISA

Mouse vascular endothelial cell growth factor (VEGF) was analyzed in serum samples using GENLISA™ ELISA kit (KLM0114). VEGF levels were quantified in serum samples of day 1 and 7 animals using an ELISA kit following the manufacturer's protocol. Briefly, standards and samples (100 µL each) were added to a 96-well plate and incubated at 37 °C for 90 min. The wells were washed and 100 µL of biotinylated anti-VEGF antibody was added, followed by 60-min incubation at 37 °C. After washing, 100 µL of Streptavidin-HRP conjugate was added and incubated for 30 min at 37 °C. Following a final wash, 100 µL of TMB substrate was added and incubated for 10 min in the dark. The reaction was stopped with 100 µL of Stop Solution, and absorbance was measured at 450 nm.

Statistics and Analysis

All statistical analyses were performed using appropriate statistical tests, depending on the type of data and its distribution. The normality of the data was assessed using the Shapiro–Wilk test to evaluate the parametric or non-parametric nature of the data followed by Bonferroni post hoc test was used to compare groups. The quantile–quantile (QQ) plots are provided as Supplementary Figs. 1, 2, 3. Non-parametric data were analyzed using the Kruskal–Wallis test followed by Dunn's post hoc test. Two-way ANOVA followed by Bonferroni post hoc test was employed for analyses involving two independent variables, such as motor coordination and grip strength assessments. For comparison between two groups, unpaired Student's *t*-test was applied. Data are presented as mean ± standard error of the mean (SEM), unless stated otherwise. Significance was defined at $p < 0.05$. For molecular analysis (gene expression and immunoblotting), a sample size of 6–8 was used while for behavioral tests, and a sample size of 7–10 mice was used. (*) indicates significant differences between the Sham group and the BCCAo or PC groups, while (#) represents significant

differences between the BCCAo group and the PC group. All statistical analyses were conducted using GraphPad Prism. Behavioral data were analyzed using Noldus EthoVision® XT 17 video tracking software.

Results

Blood Perfusion Assessment and Mortality Analysis Following UCCAo in Male and Female Mice

The rationale for conducting LDI was to confirm that UCCAo resulted in cerebral hypoperfusion after the occlusion. Blood flux measurements were recorded at three time points: before occlusion, 1 h after occlusion and 14–16 weeks after occlusion (Fig. 3). LDI at the pre-occlusion stage provided baseline measurements of cerebral blood flow. After rUCCAo, notable reduction in blood perfusion was observed at 1-h post-occlusion in both male and female animals, confirming the successful induction of cerebral hypoperfusion. Importantly, this reduced blood flux persisted even at 14–16 weeks post-occlusion, further validating the development of CCH. In the BCCAo and PC group, mortality rates were higher in males. Notably, PC reduced mortality in both male and female animals compared to the respective day-specific BCCAo group. The higher mortality observed in the 7-day post-surgery cohorts reflects cumulative deaths recorded up to day 7, rather than mortality confined to a single time point.

Neurodeficit Score Analysis in Male and Female Mice Groups Following UCCAo and PC

On day 1, one-way ANOVA in males (Fig. 4A) revealed a significant difference among the groups [$F(2, 21) = 35.61$, $p < 0.0001$]. Bonferroni's post hoc comparisons demonstrated that the BCCAo had significantly higher NDS compared to both the sham (mean difference = −1.500, $p < 0.0001$) and PC group ($p < 0.0001$). No significant difference was observed between the sham and PC groups ($p = 0.1666$). On day 7 in males (Fig. 4C), Kruskal–Wallis test was performed which revealed significant differences in median NDS among the groups [$H(2) = 14.52$, $p = 0.0007$]. Dunn's post hoc test showed that the BCCAo group exhibited significantly higher NDS compared to the sham group ($p = 0.0005$). However, there were no significant differences between the sham and PC groups ($p = 0.0773$) or between the BCCAo and PC groups ($p = 0.3558$).

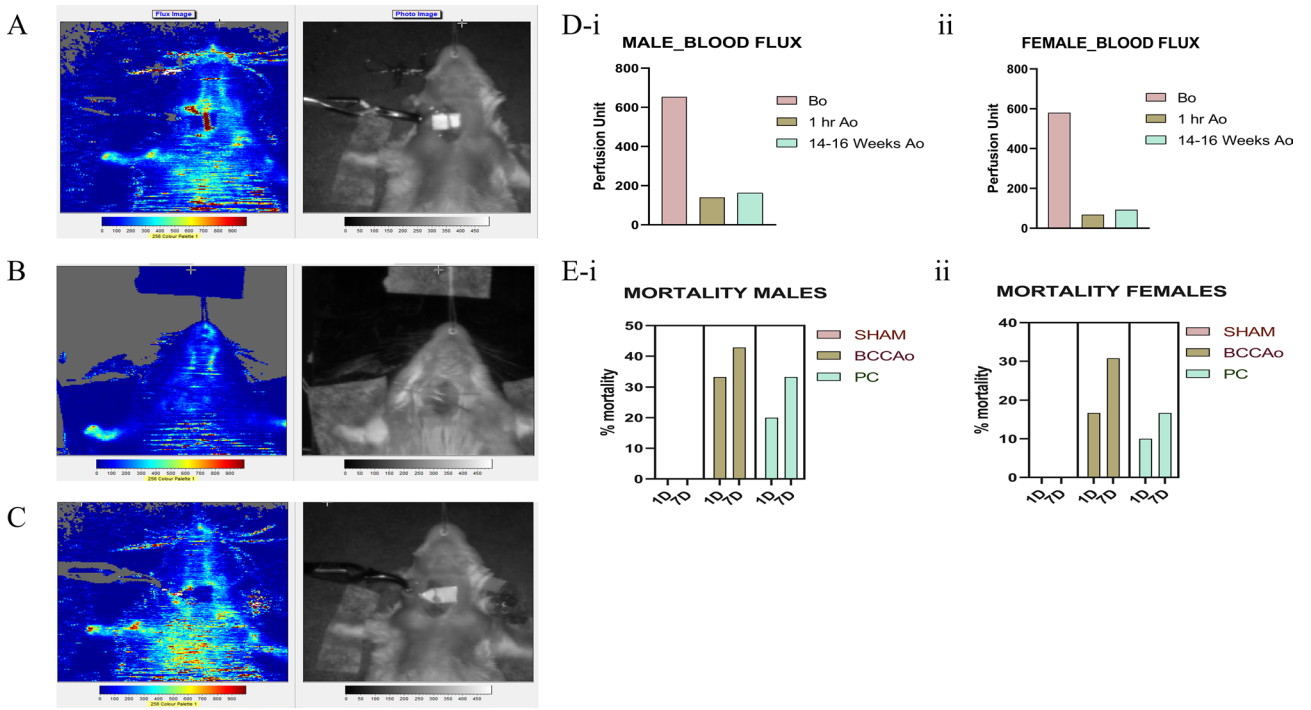

Fig. 3 Blood perfusion and mortality rates following UCCAo in male and female mice. **A** Blood perfusion in the right common carotid artery before UCCAo as measured by LDI. **B** Blood perfusion 1 h post-UCCAo showing a marked decrease in perfusion in both male and female animals. **C** Blood perfusion at 14–16 weeks post-UCCAo indicating induction of CCH. **D-i** and **D-ii** Graphical representation of blood flux over the three time points (pre-occlusion, 1-h post-occlusion and 14–16 weeks post-occlusion) for males and females, respectively. **E-i** and **E-ii** Mortality rates in males and females, respectively. Mortality rates were higher in the BCCAo group compared to the PC in both sexes

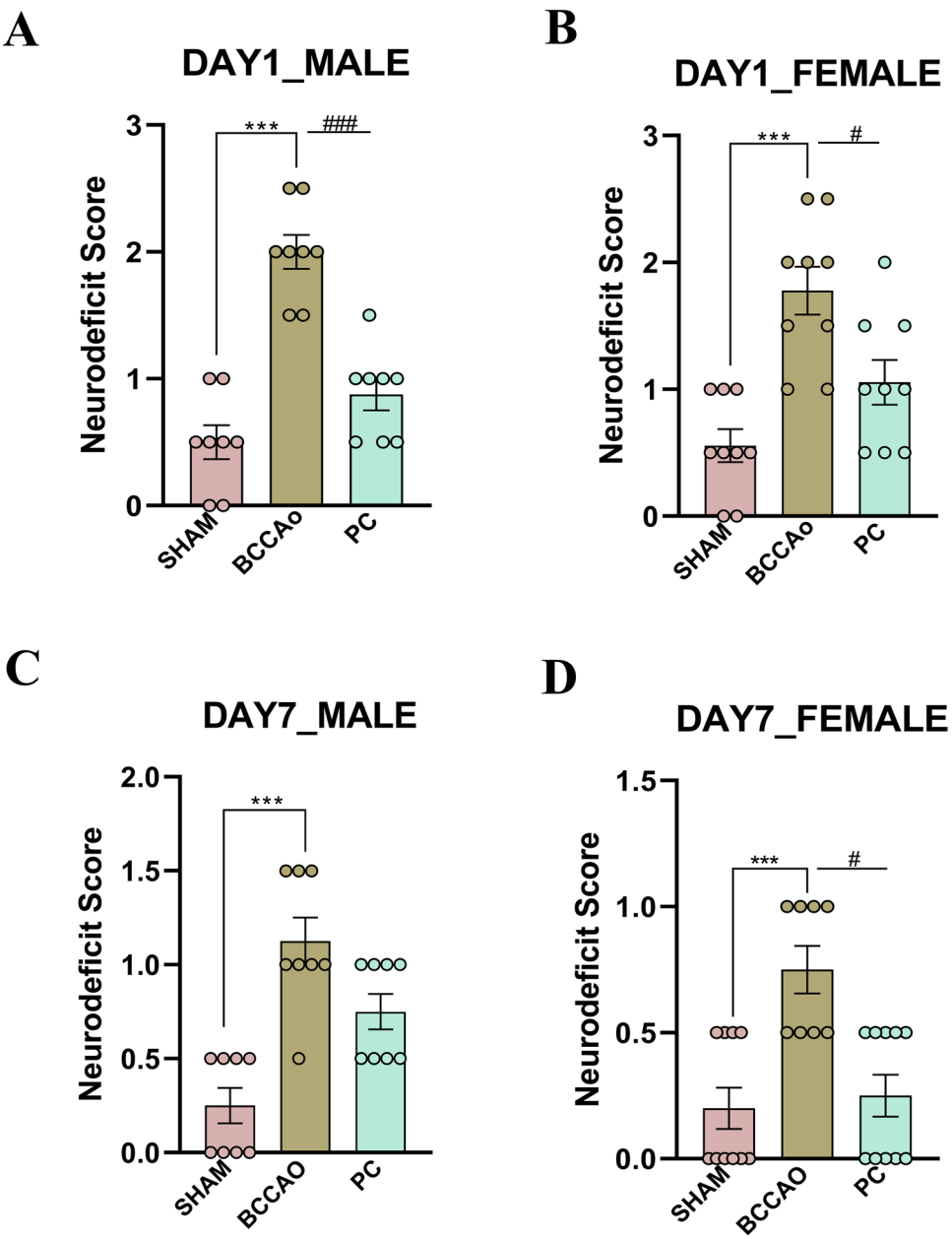

Fig. 4 Neurological-deficit score (NDS) across sham, BCCAo, and PC groups in male and female mice. **A** Day 1 NDS in male revealed significantly higher NDS in the BCCAo group compared to sham ($p < 0.0001$) and PC ($p < 0.0001$). **B** Day 1 NDS in female mice showed significantly higher NDS in the BCCAo group compared to sham ($p < 0.0001$) and PC ($p = 0.0160$). **C** Day 7 NDS in male mice revealed significantly higher NDS in the BCCAo group compared to sham ($p = 0.0005$). **D** Day 7 NDS in female mice showed significantly higher NDS in the BCCAo group compared to sham ($p = 0.0040$) and PC ($p = 0.0123$). (*) Indicates significant differences between the sham and the BCCAo or PC group; (#) Represents significant differences between the BCCAo and the PC group. Data represent the mean ± SEM, with $n = 8$ to 10 per group

On day 1 in females (Fig. 4B), one-way ANOVA revealed a significant difference among the groups [$F(2, 24) = 13.59$, $p = 0.0001$]. Post hoc Bonferroni analysis indicated that NDS was significantly higher in the BCCAo compared to the sham group ($p < 0.0001$) and the PC group ($p = 0.0160$). No significant difference was observed between the sham and PC groups ($p = 0.1333$). On day 7, in females (Fig. 4D), the Kruskal–Wallis test revealed significant differences in median NDS among the groups [$H(2) = 12.00$, $p = 0.0025$]. Dunn's post hoc test showed that the BCCAo group exhibited significantly higher NDS compared to the sham ($p = 0.0040$) and PC group ($p = 0.0123$). There was no significant difference between the sham and PC groups ($p > 0.9999$).

Assessment of Motor Coordination and Grip Strength Reveals Differential Recovery Following BCCAo and PC in Male and Female Mice

A two-way ANOVA was performed to analyze grip strength measurements in males (Fig. 5A) which revealed significant effects of group [$F(1, 42) = 15.64$, $p = 0.0003$], day [$F(2, 42) = 22.17$, $p < 0.0001$] and interaction between group and day [$F(2, 42) = 4.510$, $p = 0.0168$]. On day 1 in males, post hoc Bonferroni analysis showed that grip strength was significantly reduced in BCCAo compared to sham ($p < 0.0001$) and PC ($p = 0.0019$). Grip strength in PC was significantly reduced than in sham ($p = 0.0096$). On day 7 in males, grip strength remained significantly reduced in

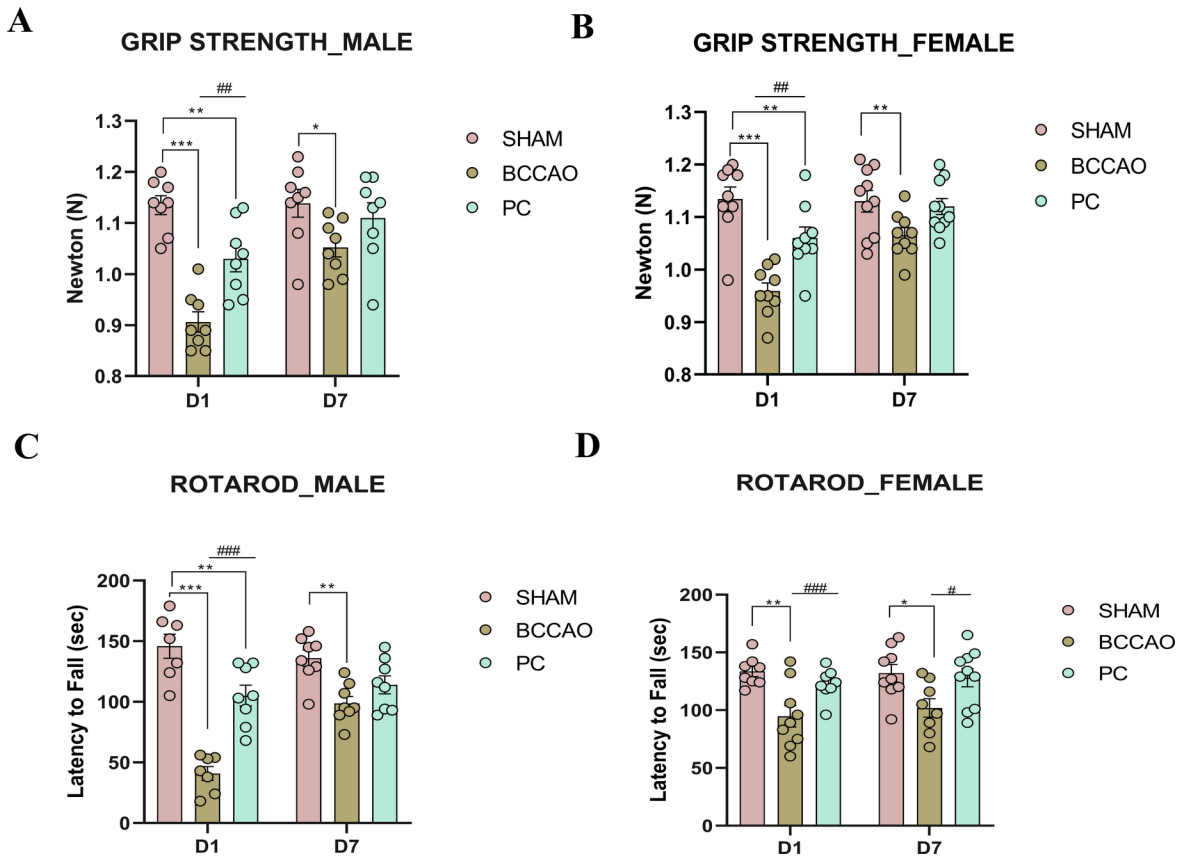

Fig. 5 Grip strength and rotarod performance in male and female mice across sham, BCCAo, and preconditioning (PC) groups on days 1 and 7. **A** On day 1, grip strength in male mice showed significant reductions in BCCAo compared to sham ($p < 0.0001$) and PC ($p = 0.0019$), with PC lower than sham ($p = 0.0096$). On day 7, grip strength remained significantly lower in BCCAo compared to sham ($p = 0.0416$). **B** In females on day 1, grip strength was significantly reduced in BCCAo compared to sham ($p < 0.0001$) and PC ($p = 0.0012$). PC group showed lower grip strength measurement compared to sham ($p = 0.0223$). On day 7, grip strength in BCCAo remained lower than sham ($p = 0.0498$). **C** Rotarod performance in males on day 1 was significantly reduced in BCCAo compared to sham ($p < 0.0001$) and PC ($p = 0.0014$), with PC higher than BCCAo ($p < 0.0001$). On day 7, BCCAo had significantly lower latency to fall than sham ($p = 0.0026$). **D** In females, rotarod performance on day 1 showed reductions in BCCAo compared to sham ($p = 0.0018$), with PC higher than BCCAo ($p = 0.0333$). 7-day group showed a significant decrease in latency to fall in BCCAo vs. sham ($p = 0.0183$). Latency was significantly higher in PC compared to BCCAo ($p = 0.0420$). (*) Indicates significant differences between the sham and the BCCAo or PC group; (#) represents significant differences between the BCCAo and the PC group. Data represent the mean ± SEM, with $n = 7$ to 10 per group

BCCAo compared to sham ($p = 0.0416$). No significant differences were observed between sham and PC ($p > 0.9999$) or BCCAo and PC ($p = 0.2826$). In females (Fig. 5B), a two-way ANOVA revealed significant effects of group [$F(1, 50) = 12.75$, $p = 0.0008$], day [$F(2, 50) = 21.27$, $p < 0.0001$], and interaction between group and day [$F(2, 50) = 4.500$, $p = 0.0160$). On day 1 females, post hoc Bonferroni analysis showed that grip strength was significantly reduced in BCCAo compared to sham ($p < 0.0001$) and PC ($p = 0.0012$). A significant reduction was also observed in sham vs. PC ($p = 0.0223$). On day 7 in females, grip strength measurements remained significantly reduced in BCCAo compared to sham ($p = 0.0498$); however, no significant differences were found between sham and PC ($p > 0.9999$) or BCCAo and PC ($p = 0.1241$).

Rotarod performance in male mice (Fig. 5C) was analyzed using two-way ANOVA which showed a significant interaction between group and day [$F(2, 40) = 10.71$, $p = 0.0002$], a significant group effect [$F(1, 40) = 9.638$, $p = 0.0035$] and a significant day effect [$F(2, 40) = 44.37$, $p < 0.0001$]. On day 1, post hoc Bonferroni tests indicated significant decrease in latency to fall in BCCAo (mean difference = 105.0, $p < 0.0001$) as well as in PC ($p = 0.0014$) when compared to sham. It was significantly higher in PC when compared to BCCAo (mean difference = − 64.27, $p < 0.0001$). Post hoc Bonferroni tests on day 7 showed significantly decreased latency to fall in BCCAo when compared to sham ($p = 0.0026$), but no significant differences between sham and PC ($p = 0.1188$) or BCCAo and PC ($p > 0.4443$). Two-way ANOVA in female mice

(Fig. 5D) revealed significant interaction [$F(2, 46) = 0.1896$, $p = 0.8279$], group effect [$F(1, 46) = 0.3993$, $p = 0.5306$], and day effect [$F(2, 46) = 11.97$, $p < 0.0001$]. Bonferroni's post hoc tests on day 1 female showed significant decrease in BCCAo ($p = 0.0018$) compared to sham. Further, significant increase in PC ($p = 0.0333$) was observed compared to BCCAo. However, there were no significant differences between sham and PC ($p > 0.9442$). Post hoc Bonferroni tests in 7-day group indicated significant decrease in latency to fall in BCCAo compared to sham ($p = 0.0183$), but no significant differences were observed between Sham and PC ($p > 0.9999$). Significant increase was observed in PC as compared to BCCAo ($p = 0.0420$).

Sex-Specific Behavioral Alterations in Open Field, Novel Object Recognition, and Y-Maze Tests Following Preconditioning and BCCAo

OFT, NORT, and Y-maze were conducted on day 7. In OFT, differential effects were observed in both male (Fig. 6A, C) and female mice (Fig. 6B, D). The male mice did not show significant differences in distance traversed across the groups [$F(2, 18) = 1.830$, $p = 0.1891$]. Post hoc tests revealed no significant differences between sham, BCCAo, and PC groups ($p > 0.05$ for all comparisons). Female mice demonstrated significant differences in the distance traversed, as indicated by one-way ANOVA results [$F(2, 19) = 9.095$, $p = 0.0017$]. Post hoc Bonferroni analysis revealed a significant reduction in distance traveled in the BCCAo group compared to sham ($p = 0.0015$) and (PC) group ($p = 0.0303$). No significant difference was observed between the sham and PC groups ($p = 0.6927$). In terms of mean velocity**,** male mice did not show significant differences [$F(2, 18) = 0.9502$, $p = 0.4052$]. In contrast, female mice displayed significant differences between the groups [$F(2, 25) = 6.633$, $p = 0.0049$]. Post hoc Bonferroni analysis showed a significant reduction in mean velocity in the BCCAo group compared to sham ($p = 0.0039$), while no significant difference was observed between sham and PC ($p = 0.1446$) or BCCAo and PC ($p = 0.4366$).

In NORT, one-way ANOVA revealed significant differences in the discriminative index (DI) in both male (Fig. 6E) and female mice (Fig. 6F). Male mice showed significant differences in DI [$F(2, 19) = 9.137$, $p = 0.0017$]. Post hoc Bonferroni's test revealed a significant decrease in the DI of the BCCAo group compared to sham ($p = 0.0015$) and PC ($p = 0.0300$). The PC group did not differ significantly from sham ($p = 0.6864$). Female mice also exhibited significant differences in DI [$F(2, 23) = 5.807$, $p = 0.0091$]. Bonferroni's post hoc analysis revealed a significant decrease in the DI of the BCCAo group compared to sham ($p = 0.0073$). However, there was no significant difference between sham and PC ($p = 0.3891$), nor between BCCAo and PC groups ($p = 0.1573$).

In Y-maze test in males (Fig. 6G), the one-way ANOVA showed no differences in % alternation [$F(2, 20) = 1.583$, $p = 0.2301$] among groups. Similarly in females, no significant differences were observed [Fig. 6H, $F(2, 23) = 0.8857$, $p = 0.4260$]. In Novel Arm test in males (Fig. 6I), the BCCAo mice spent significantly less time in the novel arm compared to sham group ($p = 0.0045$) as well as to the PC group ($p = 0.0478$). No change was observed between sham and PC ($p = 0.9534$). In females (Fig. 6J), the BCCAo group spent significantly less time in the novel arm compared to the sham group ($p = 0.0059$), while no differences were found between the sham and PC ($p = 0.4238$), or between the BCCAo and PC groups ($p = 0.1731$). In terms of the frequency of entries into the novel arm, male BCCAo mice (Fig. 6K) showed significantly fewer entries compared to the sham group ($p = 0.0051$). PC group showed significantly less frequency compared to sham group ($p = 0.0430$). No differences were observed between BCCAo and PC ($p > 0.9999$) while in female mice (Fig. 6L) in the BCCAo group significantly, fewer entries were observed compared to the sham group ($p = 0.0125$) as well as to PC ($p = 0.0028$). No differences were observed between sham and PC ($p > 0.9999$).

Differential Glial Activation in the Striatum Following Ischemic Preconditioning

To investigate the effects of IPC on astrocytic and microglial activation, we performed immunofluorescence analysis of GFAP (Fig. 7) and IBA1 (Fig. 8) expression in the striatum.

Reactive Astrocytes Exhibit Reduced Hypertrophy in Preconditioned State

In males, a one-way ANOVA revealed a significant difference in number of GFAP-positive cells between groups [$F(2, 6) = 12.85$, $p = 0.0068$]. The BCCAo group exhibited significantly higher GFAP-positive cells compared to the sham group ($p = 0.0084$). The difference between PC and BCCAo was statistically significant ($p = 0.0316$) indicating reduced GFAP in PC. In females, one-way ANOVA revealed a significant difference in number of GFAP-positive cells between groups [$F(2, 6) = 30.31$, $p = 0.0007$]. The BCCAo group exhibited significantly higher number of GFAP-positive cells compared to the sham group ($p = 0.0008$). In the PC group, GFAP expression was moderately elevated compared to the sham group though not reaching significance, but significantly lower than in the BCCAo group suggesting reduced astrocytic activation ($p = 0.0049$).

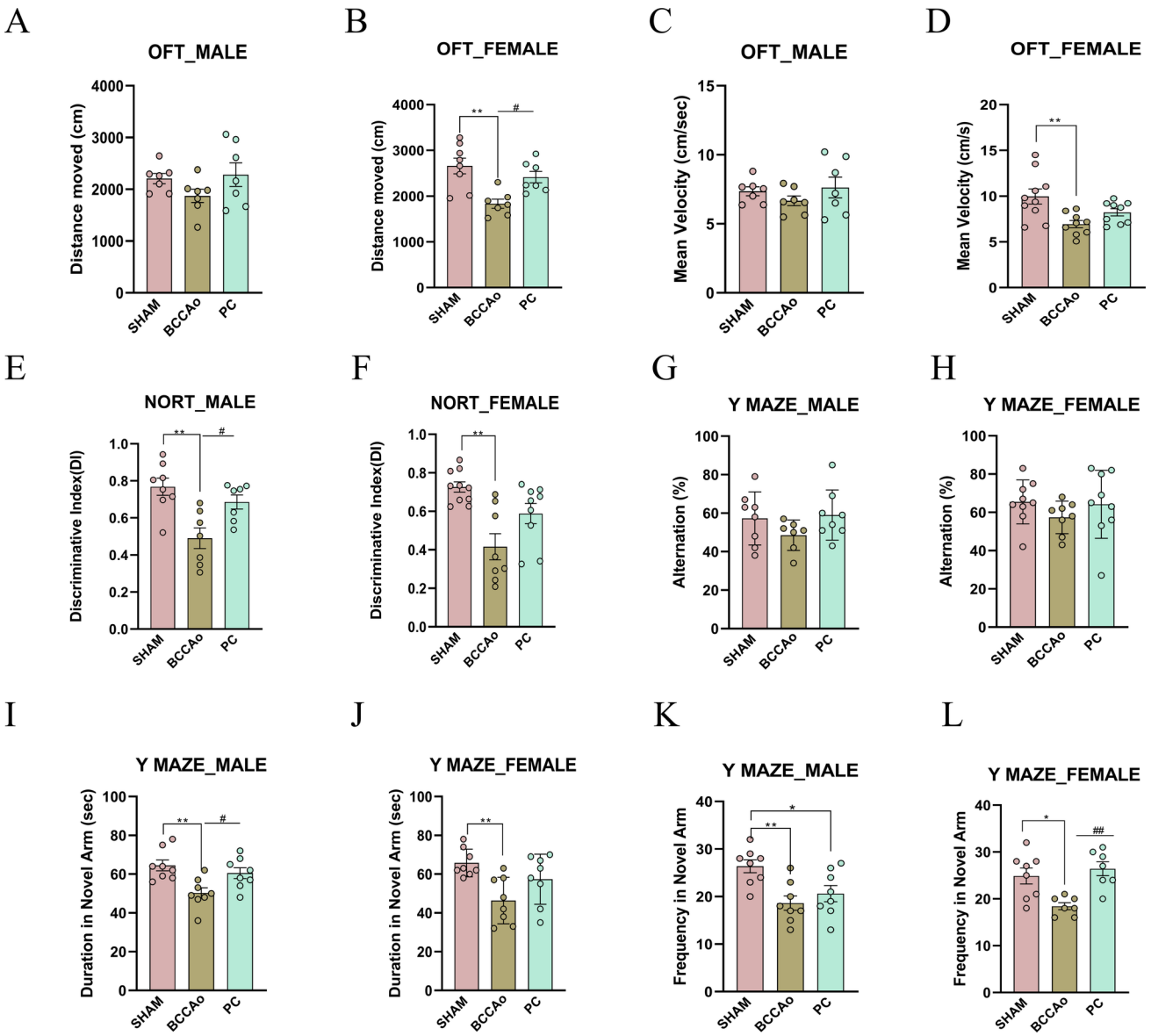

Fig. 6 Motor and cognitive behavior assessments following BCCAo and preconditioning. **A** OFT male distance moved: no significant differences were observed between sham, BCCAo, and PC groups. **B** OFT female distance moved: the BCCAo group showed reduced distance compared to sham ($p=0.0015$) and PC ($p=0.0303$). **C** OFT male mean velocity: no significant differences were observed across groups. **D** OFT female mean velocity: the BCCAo group exhibited lower velocity compared to sham ($p=0.0039$). **E** NORT male DI: the BCCAo group had reduced DI compared to sham ($p=0.0015$) and PC ($p=0.0300$). **F** NORT female DI: the BCCAo group showed reduced DI compared to sham ($p=0.0073$). **G** Y-Maze male % alternation: no significant differences were observed. **H** Y-Maze female % alternation: no significant differences were observed. **I** Y-Maze male duration in novel arm: the BCCAo group spent less time in the novel arm compared to sham ($p=0.0045$) and PC ($p=0.0478$). **J** Y-Maze female duration in novel arm: the BCCAo group spent less time in the novel arm compared to sham ($p=0.0059$). **K** Y-Maze male frequency to novel arm: the BCCAo group entered the novel arm less frequently than sham ($p=0.0051$). PC showed fewer entries compared to sham ($p=0.0430$). **L** Y-Maze female frequency to novel arm: the BCCAo group entered the novel arm less frequently than sham ($p=0.0125$), while PC showed higher entries compared to BCCAo ($p=0.0028$). (*) Indicates significant differences between the sham and the BCCAo or PC group; (#) represents significant differences between the BCCAo and the PC group. Data represent the mean ± SEM, with $n=7$ to 10 per group

Microglial Activation is Dampened in Preconditioned Male Mice

In males, a one-way ANOVA ($F(2, 6)=39.52$, $p=0.0004$) revealed that BCCAo exhibited significantly increased IBA1 expression compared to sham ($p=0.0003$). PC exhibited significantly reduced IBA1 expression compared to BCCAo ($p=0.0059$). However, when compared with sham, PC showed significantly higher ($p=0.0335$) expression. In females ($F(2, 6)=10.06$, $p=0.0121$), a one-way ANOVA revealed significant

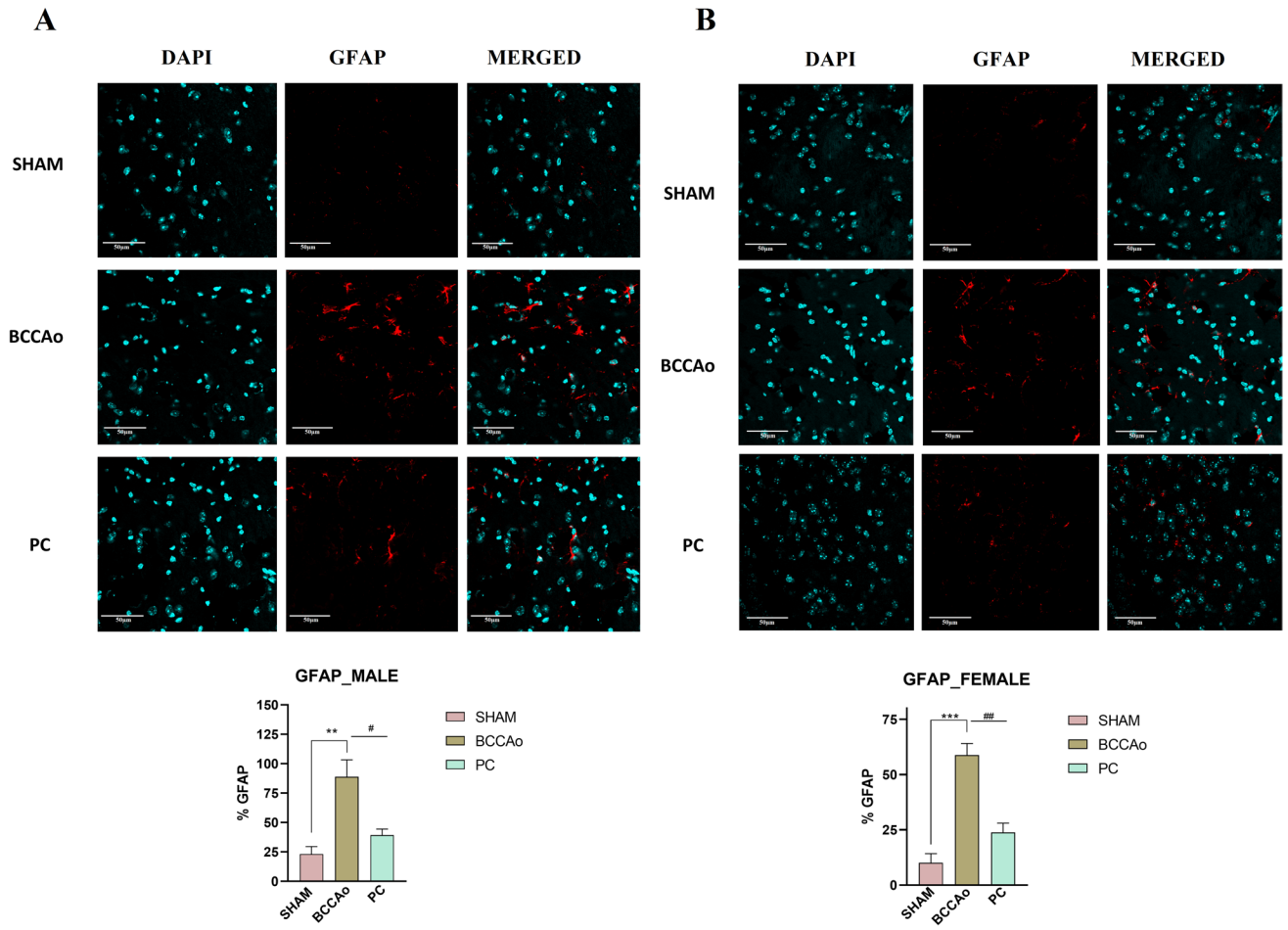

Fig. 7 GFAP immunostaining in the striatum. Representative images showing astrocytic activation (GFAP) in the striatum of male (**A**) and female (**B**) mice. Images were captured at × 60 magnification using an Olympus FV 10i confocal microscope. BCCAo group exhibits significantly increased astrocytic activation in both males and females. The preconditioned (PC) group shows moderately elevated GFAP expression compared to the sham group, with significantly lower number of GFAP-positive cells than the BCCAo group, indicating reduced astrocytic activation. Statistical analysis revealed significant differences between the sham and BCCAo groups ($p = 0.0084$, males; $p = 0.0008$, females) and between the BCCAo and PC groups ($p = 0.0316$, males; $p = 0.0049$, females). (*) Indicates significant differences between the sham and the BCCAo or PC group; (#) represents significant differences between the BCCAo and the PC group. Data represent the mean ± SEM, with $n = 3$ per group

differences in number of IBA1-positive cells between groups. The BCCAo group exhibited increased IBA1-positive cells compared to the sham group ($p = 0.0131$). While there was a trend toward reduced microglial activation in PC compared to the BCCAo group, it was, however, not statistically significant ($p = 0.0966$). Furthermore, no significant difference was observed between sham and PC ($p = 0.4406$).

Gene expression analysis reveals sex-divergent transcriptional responses to CCH-induced preconditioning

One-way ANOVA was performed followed by post-hoc Bonferroni corrections for statistical analysis of gene expression studies. In males, *Hif1a* levels (Fig. 9A) showed a significant increase in the BCCAo group compared to the sham group (adjusted p-value < 0.0001); however, no significant difference was observed between the BCCAo and PC groups ($p = 0.9770$). Significant increase was observed in PC compared to sham groups ($p = < 0.0001$). In females, BCCAo also exhibited significantly elevated *Hif1a* levels (Fig. 9B) compared to sham (adjusted p value $= 0.0378$). PC did not significantly differ from either sham ($p = 0.6615$) or BCCAo ($p = 0.4228$) in females, suggesting potential sex-dependent differences in ischemic adaptation and preconditioning efficacy. In males, *Becn1* levels (Fig. 9C) were significantly higher in the PC compared to sham (adjusted p-value $= 0.0148$), but no significant difference was observed between sham and BCCAo ($p = 0.0988$). This suggests that PC specifically enhances autophagic activity. No

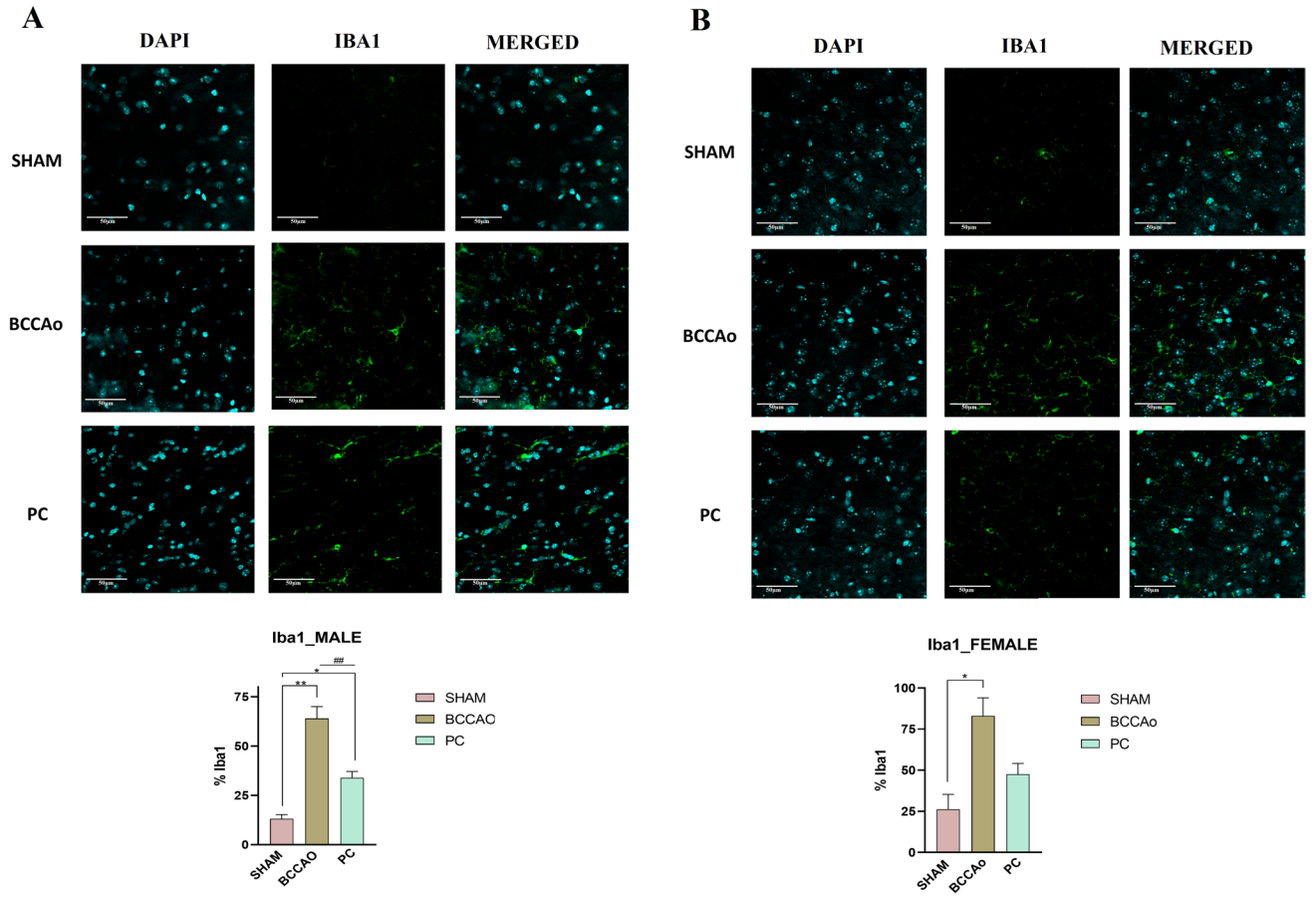

Fig. 8 IBA1 immunostaining in the striatum. Representative images showing microglial activation (IBA1) in the striatum of male and female mice. Images were captured at × 60 magnification using an Olympus FV 10i confocal microscope. The sham group shows resting microglia while the BCCAo group exhibits significantly increased microglial activation, with amoeboid morphology in both males and females. The preconditioned (PC) group displays an intermediate morphology, transitioning toward a more ramified phenotype. Statistical analysis revealed significant differences between the sham and BCCAo groups ($p = 0.0003$, males; $p = 0.0131$, females) and between the BCCAo and PC groups ($p = 0.0059$, males; $p = 0.0966$, females). In males, PC showed significantly higher expression than sham ($p = 0.0335$). (*) Indicates significant differences between the sham and the BCCAo or PC group; (#) represents significant differences between the BCCAo and the PC group. Data represent the mean ± SEM, with $n = 3$ per group

significant difference was observed between BCCAo and PC ($p > 0.9999$). In females *Becn1* (Fig. 9D) expression was significantly elevated in both BCCAo and PC groups compared to sham (adjusted p values = 0.0141 and < 0.0001, respectively); however, this change was more pronounced in PC. The BCCAo vs. PC comparison could not approach significance ($p = 0.0548$), yet implying a trend toward increased autophagy in PC females.

Male *Il1b* levels (Fig. 9E) were significantly elevated in the BCCAo group compared to sham (adjusted p value = 0.0116). PC exhibited no significant difference when compared to sham ($p = 0.1739$) or to BCCAo ($p = 0.6706$). In females, *Il1b* levels (Fig. 9F) were significantly higher in BCCAo compared to sham (adjusted p value = 0.0382) with PC showing no significant difference ($p = 0.793$). In males, *Sox2* (Fig. 9G) expression was significantly lower in BCCAo compared to sham (adjusted p value = 0.0147). *Sox2* expression was significantly elevated in PC compared to BCCAo (adjusted p value = 0.0002), while no significant differences were observed between sham and PC ($p = 0.1848$). No notable variations in Sox2 expression were observed in females (Fig. 9H) between the different groups. In males, *Il6* levels (Fig. 9I) were significantly elevated in the BCCAo group compared to sham (adjusted p value = 0.0003). PC exhibited no significant difference when compared to BCCAo ($p = 0.2285$) but remained significantly higher than sham ($p = 0.0271$). In females, *Il6* levels (Fig. 9J) were significantly higher in BCCAo compared to sham (adjusted p value < 0.0001), with PC also showing significantly higher levels than sham ($p = 0.0004$) but no significant difference from BCCAo ($p > 0.9999$).

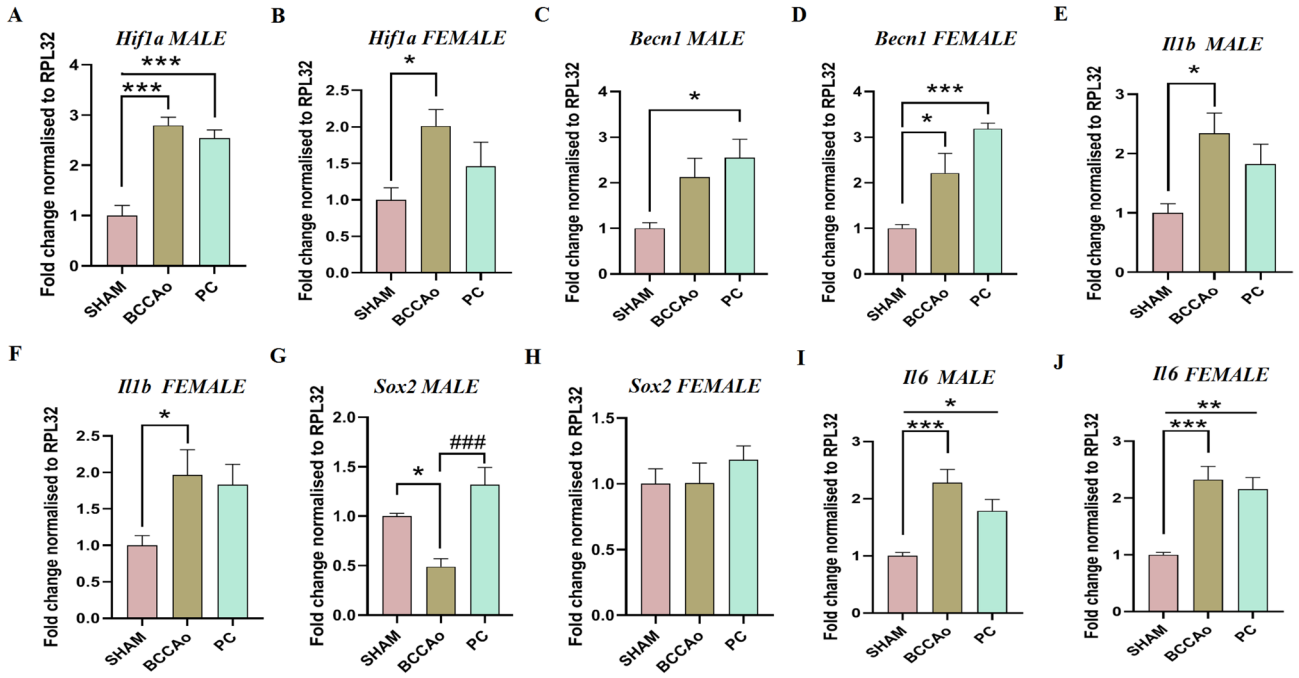

Fig. 9 Sex-specific expression patterns of *Hif1a*, *Becn1*, *Il1b,* and ***Sox2*** in sham, BCCAo, and PC. In males, *Hif1a* levels (**A**) were significantly elevated in the BCCAo group compared to sham (adjusted p-value < 0.0001), while PC showed significantly higher levels compared to sham ($p < 0.0001$). In females (**B**), BCCAo exhibited significantly elevated *Hif1a* levels compared to sham ($p = 0.0378$). For *Becn1*, males (**C**) showed significantly higher expression in PC versus sham (adjusted p-value = 0.0148), with no differences between other groups. In females (**D**), *Becn1* expression was significantly elevated in both BCCAo and PC compared to sham ($p = 0.0141$ and < 0.0001, respectively). Male *Il1b* levels (**E**) were significantly elevated in BCCAo compared to sham ($p = 0.0116$). Similarly, in females (**F**), *Il1b* levels were significantly higher in BCCAo compared to sham ($p = 0.0382$). For *Sox2*, males (**G**) showed significantly reduced expression in BCCAo versus sham ($p = 0.0147$), significantly elevated expression in PC versus BCCAo ($p = 0.0002$). No significant differences in *Sox2* expression were observed among female groups (**H**). Data represent the mean ± SEM, with $n = 6$–8 per group. In males, *Il6* levels (**I**) were significantly elevated in the BCCAo group compared to sham (adjusted p-value = 0.0003), while PC remained significantly higher than sham ($p = 0.0271$). In females (**J**), BCCAo exhibited significantly elevated *Il6* levels compared to sham ($p < 0.0001$), with PC also showing significantly higher levels than sham ($p = 0.0004$). (*) Indicates significant differences between the sham and the BCCAo or PC group; (#) represents significant differences between the BCCAo and the PC group. Data represent the mean ± SEM, with $n = 6$ to 8 per group

Preconditioning Mediates Translational Regulation of Synaptic Strengthening and Neurotrophic Responses

PSD-95, synaptophysin and BDNF are critical markers of synaptic health, neuronal plasticity, and neuroprotection. By comparing the levels of striatal proteins between the BCCAo and PC groups at day 1 post-surgery, we aimed to assess the neuroprotective and synaptic preservation effects of preconditioning. For SYN, BDNF, and PSD-95 expression levels, statistical analyses revealed significant differences between the PC and BCCAo groups. Males exhibited a highly significant increase in BDNF levels (Fig. 10A) in the PC group compared to BCCAo ($p < 0.0001$). Females (Fig. 10B) also showed a significant increase ($p = 0.0425$) in BDNF levels. In males (Fig. 10C) a significant increase was observed ($p = 0.0101$) in SYN, whereas in females (Fig. 10D) the difference was not significant ($p = 0.8178$). Similarly, PSD-95 levels (Fig. 10E, F) were significantly elevated in both males ($p = 0.0002$) and females ($p < 0.0001$).

CCH Preconditioning Enhances VEGF Expression

The serum VEGF levels were significantly elevated in the PC group compared to the sham and BCCAo groups at day 1 post-surgery in both male and female cohorts, indicating an early response to preconditioning. In males (Fig. 11A) at day 1 VEGF levels in the PC group was significantly higher than both sham ($p = 0.0003$) and BCCAo ($p = 0.0152$). By day 7, VEGF levels in the BCCAo group were significantly elevated compared to sham ($p = 0.0026$) and the PC group also showed an increase relative to sham ($p = 0.0122$) indicating a sustained response. In females (Fig. 11B), VEGF levels in the PC group at day 1 were significantly higher than in both the sham ($p < 0.0001$) and BCCAo ($p = 0.0035$) groups, whereas no significant difference was observed between sham and BCCAo groups.

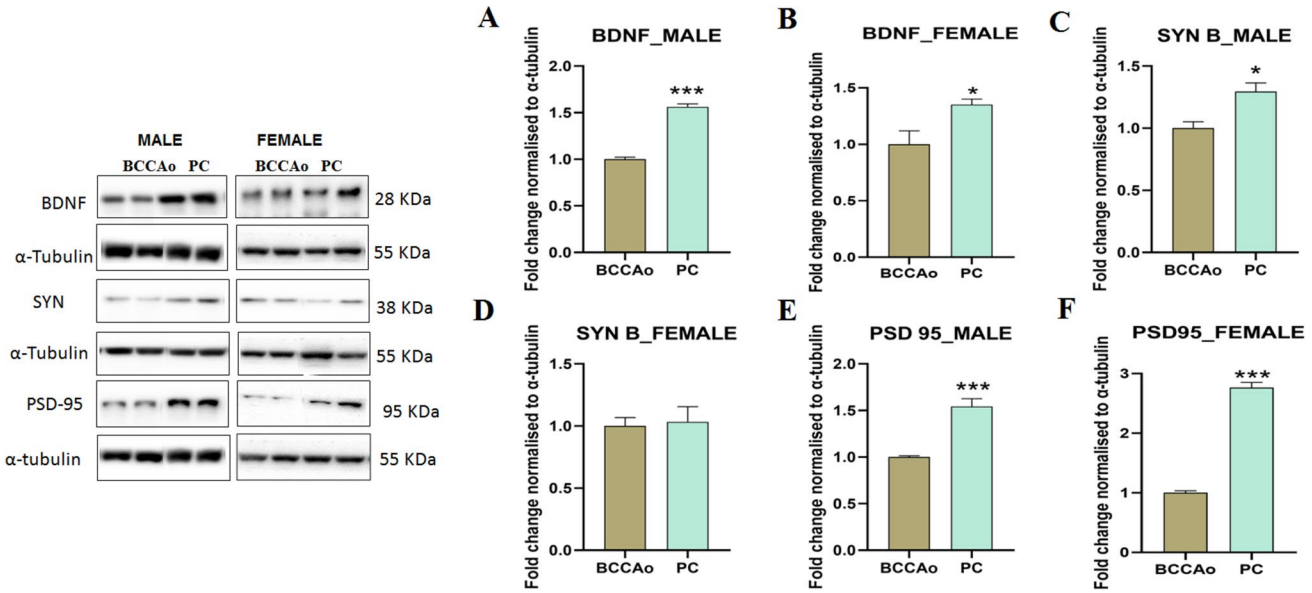

Fig. 10 Western blot analysis of striatal protein expression in males and females following PC and BCCAo**.** A In males significant increase in BDNF expression in the PC group was observed compared to BCCAo ($p < 0.0001$). B In females significant increase in BDNF expression in the PC group compared to BCCAo ($p = 0.0425$) was observed. C SYN in males significantly increased in the PC group compared to BCCAo ($p = 0.0101$). D SYN female: no significant difference in SYN expression between PC and BCCAo groups ($p = 0.8178$). E PSD-95 in males was increased significantly in the PC group compared to BCCAo ($p = 0.0002$) while in females (F) as well PSD-95 expression in the PC group increased compared to BCCAo ($p < 0.0001$). Data are presented as mean ± SEM. Data represent the mean ± SEM, with $n = 6$–7 per group

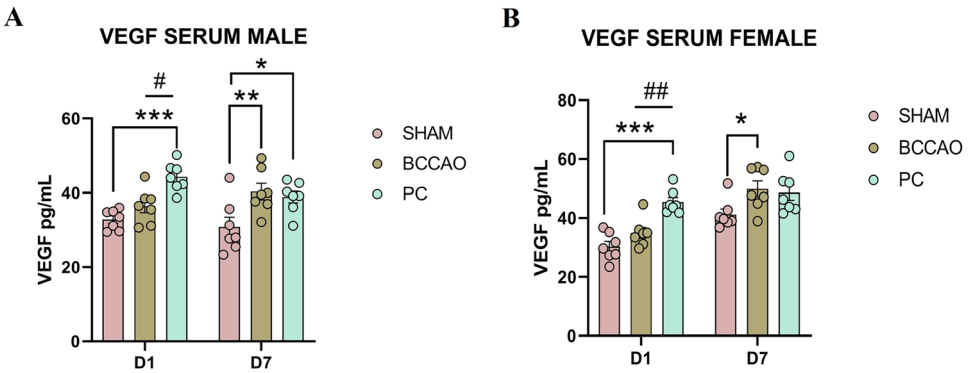

Fig. 11 Serum VEGF levels in males (**A**) and females (**B**) show significant time and group-specific changes. In males (**A**), on day 1, VEGF levels in the PC group were significantly higher than those in the sham ($p = 0.0003$) and BCCAo ($p = 0.0152$) groups. By day 7, VEGF levels in the BCCAo group showed a significant increase compared to sham ($p = 0.0026$), while the PC group also exhibited elevated levels relative to sham ($p = 0.0122$). In females (**B**), on day 1, the PC group displayed significantly elevated VEGF levels compared to both sham ($p < 0.0001$) and BCCAo ($p = 0.0035$). By day 7, VEGF levels in the BCCAo group were significantly higher than sham ($p = 0.0184$). (*) Indicates significant differences between the sham and the BCCAo or PC group; (#) represents significant differences between the BCCAo and the PC group. Data represent the mean ± SEM, with $n = 7$ per group

By day 7, VEGF levels in the BCCAo group were significantly elevated compared to sham ($p = 0.0184$), while the PC group levels remained comparable to sham suggesting normalization in preconditioned females.

Discussion

Preconditioning represents a compelling concept in neuroscience, where controlled, mild ischemic events can train the brain to build resilience against subsequent severe ischemic injuries. In this study, we explored this idea

within the context of CCH, a condition characterized by sustained reduction in cerebral blood flow. CCH is widely recognized for its long-term detrimental effects on brain health, often contributing to VaD. Here, we investigated a novel possibility: could chronic, mild hypoperfusion itself act as a form of preconditioning, enhancing the brain's resilience against severe ischemic insults such as acute stroke? In rats BCCAo is commonly used to simulate CCH as their well-developed collateral circulation and robust circle of Willis compensates bilateral carotid artery occlusion (Choi et al. 2016; Bhat and Kumar 2022). Unlike rats mice possess a poorly developed circle of Willis and reduced collateral blood flow resulting in rapid and severe ischemia making BCCAo in mice suitable for studying acute global ischemic stroke (Kelly et al. 2001; Soares et al. 2013; Lee et al. 2022). Building upon these insights our study aimed to develop a preconditioning model utilizing UCCAo-induced CCH as a preconditioning stimulus to induce a state of ischemic tolerance. The UCCAo creates a controlled state of CCH by selectively reducing blood flow to one hemisphere, allowing the contralateral brain to adapt to sublethal hypoperfusion. BCCAo was employed as a severe ischemic insult to simulate transient global cerebral ischemia (tGCI). Importantly, 22–25 weeks old CD1 mice were procured which aged around 9 months at the time of final surgery thus corresponding to middle age in mice. In the BCCAo model used in our study, which induces acute global ischemia, there is often some degree of recovery by day 7. This recovery can obscure the acute effects of preconditioning, making day 1 a more informative timepoint for studying the immediate molecular responses. Thus, while behavioral assessments were conducted at both days 1 and 7, the molecular analysis focused on data from day 1 which provided essential insights into the early protective mechanisms induced by preconditioning.

Striatum, a critical subcortical structure was selected for investigation in our experiments due to its established vulnerability to ischemic insult following cerebral ischemia (Akinmoladun et al. 2021; Xiao et al. 2021; Santos et al. 2023). It plays a central role in motor control, cognitive functions and reward processing making it a key target for evaluating the neuropathological and functional consequences of ischemia(Laforce Jr and Doyon 2001; Bhanji and Delgado 2014). Previous studies have demonstrated that BCCAo induces significant metabolic and structural changes in the striatum including neuronal damage, astrocytic activation, epigenetic dysregulations and alterations in neurotransmitter systems (de Aguiar et al. 2021; Radhakrishnan et al. 2024b). This vulnerability makes the striatum a critical site for investigating CCH preconditioning-induced ischemic resiliency. By incorporating sex as a biological variable, we sought to determine whether the neuroprotective potential of CCH is modulated by sex-specific mechanisms. Emerging evidences indicate that biological sex plays a critical role in ischemic brain injury and recovery (Shansky and Murphy 2021; Burton et al. 2024; Radhakrishnan et al. 2024a).

LDI confirmed significant cerebral hypoperfusion immediately following UCCAo in both male and female mice with minimal recovery of blood flow over 14–16 weeks. This may be due to vascular remodeling or collateral circulation development as evident from other studies (Burnier et al. 2016; Halder et al. 2018). However, perfusion levels did not return to baseline indicating sustained cerebral hypoperfusion. Interestingly mortality analysis revealed sex-specific differences, with male mice exhibiting higher mortality in the BCCAo and PC group compared to females. Preconditioning significantly reduced mortality rates in both the sexes further supporting its neuroprotective role. The sex-dependent mortality patterns may be attributed to inherent differences in vascular architecture, hormonal influences or ischemic tolerance thresholds. NDS revealed critical insights into the efficacy of IPC. On day 1 post-surgery, BCCAo mice exhibited severe neurodeficits compared to sham controls, consistent with the acute neurological impact of transient global ischemia (Wahul et al. 2018). In contrast, preconditioned mice showed significantly lower NDS indicating partial neuroprotection. By day 7, the neurodeficits in preconditioned mice were no longer significantly different from the sham group in both sexes, suggesting continued recovery and resilience mediated by preconditioning, aligning more closely with baseline levels over time.

Behavioral assessments including OFT, rotarod and GST tests, provided evidence of differential locomotor activity, motor coordination and forearm grasping ability respectively. In the rotarod and GST tests, preconditioned mice demonstrated partial recovery of motor coordination and strength by day 7, with values approaching those of sham controls. In contrast, BCCAo mice exhibited persistently reduced performance in rotarod and grip strength tests highlighting the debilitating effects of global ischemia. In males, the OFT indicated no significant differences across all groups, while female mice showed more pronounced effects in the BCCAo group. Cognitive tests, including NORT and Y-maze revealed significant impairments in recognition memory in the BCCAo group for both sexes, consistent with the striatal vulnerability to ischemia. Preconditioned males exhibited improved cognitive performance compared to BCCAo males, whereas PC females did not show significant recovery in the discriminative index. This sex divergence may be attributed to hormonal influences or the more pronounced locomotor impairments observed in BCCAo females, as evidenced by the OFT results. In the Y-maze test, the BCCAo group demonstrated reduced time spent in the novel arm, indicative of impaired spatial

memory. Preconditioning mitigated these deficits, with more pronounced improvements observed in males.

Astrocytes the most abundant glial cells in the central nervous system (CNS) play a critical role in maintaining neuronal homeostasis and supporting neuroprotection under physiological conditions. However, during pathological events such as ischemia, the upregulation of GFAP, a hallmark of reactive astrogliosis, often signifies impaired neuronal homeostasis (Pekny et al. 2019; Stadler et al. 2022). Immunofluorescence staining for GFAP revealed distinct patterns of astroglial activation across experimental groups in the striatum for both sexes. In the sham group, astrocytes displayed morphology of non-reactive astrocytes. In the BCCAo group, a significant increase in number of GFAP-positive cells was observed in both males and females indicating pronounced hypertrophy of astrocytic processes, suggesting robust astroglial activation in response to acute ischemic injury. In the PC group, GFAP expression was moderately elevated compared to the sham group but significantly lower than in the BCCAo group for both sexes, where astrocytes exhibited a less hypertrophic morphology with a more organized pattern of GFAP-positive processes. Overall, the results suggest that preconditioning mitigates excessive astroglial activation in both sexes, potentially promoting a neuroprotective astrocytic phenotype.

Microglia, the CNS's resident immune cells, play a dual role in either exacerbating damage or promoting repair, depending on their activation state. In stroke models, hyperactivation of microglia leads to the release of pro-inflammatory cytokines, reactive oxygen species (ROS) and nitric oxide, amplifying neuronal damage (Weinstein et al. 2009; Lier et al. 2021). IBA1 immunostaining in the BCCAo group of both sexes exhibited marked increases in microglial activation. Activated microglia showed a characteristic amoeboid morphology, indicative of pro-inflammatory activation. Interestingly, in the preconditioning group, microglia displayed an intermediate morphology, transitioning toward a more ramified phenotype in both males and females, suggesting a shift toward a less pro-inflammatory state. In males, the PC showed a significant reduction in IBA1-positive cells compared to the BCCAo group, although IBA1 expression remained higher than in the sham group. In females, the preconditioning group exhibited a trend toward reduced microglial activation, with fewer IBA1-positive cells compared to the BCCAo group, but the difference between the preconditioning and BCCAo groups did not reach statistical significance. Further histological analysis of striatal brain sections using hematoxylin and eosin (H&E) staining (Supplementary Fig. 4) indicated subtle ischemic damage in the BCCAo group and early structural improvements in the preconditioning group.

Gene expression analyses revealed distinct differences in the regulation of key biomarkers involved in ischemic tolerance. Both sexes showed elevated levels of *Hif1a*, a marker of hypoxic adaptation, in response to BCCAo. Preconditioning normalized *Hif1a* levels in females, while males exhibited a less pronounced effect, suggesting sex-specific regulatory mechanisms in hypoxia-inducible pathways. Additionally, *Becn1* associated with autophagy was upregulated in males following preconditioning, which likely contributed to enhanced protective autophagic activity. In females, *Becn1* was elevated in both BCCAo and preconditioning groups, potentially reflecting estrogen's role in promoting autophagy. Preconditioning reduced *Il1b* levels in both males and females indicating an attenuation of inflammatory responses.

Preconditioning reduced *Il1b* levels in both males and females, indicating an attenuation of inflammatory responses. The reduction in *Il1b* levels aligns with its role as a key mediator of acute inflammatory injury, and its dampening likely contributes to the neuroprotective effects of preconditioning. However, *Il6* levels remained elevated in the PC group compared to sham in both sexes, with no significant reduction compared to BCCAo. While it is traditionally considered a pro-inflammatory cytokine, *Il6* also has well-documented neuroprotective and regenerative properties. Elevated *Il6* levels in the PC group, despite preconditioning, may reflect its role in promoting tissue repair, cellular survival, and adaptive immune modulation (Erta et al. 2012). The differential response in *Sox2* expression between sexes further emphasizes sex-specific neurogenic or reparative processes, with males showing normalization of *Sox2* levels post-preconditioning, whereas females displayed no significant changes.

To emphasize the protective and adaptive mechanisms induced by PC against ischemic damage immunoblotting was conducted exclusively between the BCCAo and PC groups, focusing on the differential effects of preconditioning. In this study, PC significantly increased the expression of synaptic proteins like PSD-95, synaptophysin (SYN), and BDNF, aligning with prior research that highlights the ability of preconditioning to promote synaptic plasticity and protect neuronal function. In males, PC notably elevated PSD-95, SYN, and BDNF levels, with the most pronounced effects on PSD-95 and BDNF, suggesting that preconditioning not only preserves synaptic integrity but also enhances synaptic strength by increasing neurotrophic support. This is consistent with previous investigations on IPC (Neumann et al. 2015; Geng et al. 2021; Jeong et al. 2024). In females, the effects were also observed, particularly for BDNF and PSD-95, though the response in SYN expression was less pronounced. These findings further support the notion that preconditioning can induce adaptive neuroprotective mechanisms, boosting synaptic strength and plasticity, which is critical for recovery and minimizing long-term cognitive deficits after ischemia.

To investigate angiogenic response to preconditioning, we assessed VEGF levels in serum. VEGF levels were significantly elevated in the PC group compared to both sham and BCCAo groups in both sexes, indicating a robust and early pro-angiogenic response to preconditioning These findings suggest that IPC elicits a robust and early pro-angiogenic response in both sexes, with notable differences in the resolution of VEGF levels over time. The normalization of VEGF in preconditioned females by day 7 may reflect a more efficient adaptive response. In contrast, the sustained VEGF elevation in males may indicate prolonged angiogenic activity, which could contribute to differences in vascular remodeling and ischemic resilience. Our results indicating increased VEGF levels on IPC are consistent with previous findings (Kawata et al. 2001; Ueno et al. 2016). The behavioral and molecular experiments in this study were planned to assess and confirm the neuroprotective effects of UCCAo mediated CCH-induced preconditioning. The results collectively demonstrate that PC mice exhibited resilience to global stroke-induced ischemic damage. This study identified significant sex-specific differences in the response to ischemic preconditioning (IPC) at behavioral and molecular level. While these findings emphasize the importance of sex as a biological variable in ischemic resilience, our study did not explore the mechanistic basis of these differences. Further research is needed to uncover the underlying mechanisms. Overall, this model provides a robust platform for investigating the mechanisms underlying preconditioning and holds significant promise for advancing our understanding of neuroprotective and therapeutic strategies for mitigating ischemic damage.

Conclusion

This study successfully developed and validated an IPC model using UCCAo to induce a state of ischemic tolerance and demonstrated its efficacy in mitigating the effects of BCCAo-induced transient global cerebral ischemia. The combination of behavioral, histological, and molecular analyses provided a comprehensive framework to evaluate the efficacy of the preconditioning model. Key findings highlight the ability of preconditioning to reduce mortality, attenuate neurodeficits, and enhance recovery in both male and female mice. This study particularly focused on glial activation, neuroinflammation, and functional recovery. The results demonstrate that UCCAo preconditioning can induce ischemic tolerance leading to reduced neuroinflammation and improved functional recovery following BCCAo. The dual modulation of astrocytic and microglial activation emphasizes the protective effects of CCH preconditioning. This study indicates that preconditioning may confer sex-specific differential ischemic tolerance thresholds potentially linked to molecular mechanisms that warrant further investigation. Our understanding of the underlying mechanisms of ischemic resilience will contribute to the development of targeted therapeutic interventions for stroke and vascular cognitive impairment.

Supplementary Information The online version contains supplementary material available at https://doi.org/10.1007/s10571-025-01547-z.

Acknowledgements The authors extend their sincere gratitude to B. Jyothi Lakshmi and N. Sai Ram for their diligent care and maintenance of the animals throughout the study at CCMB Animal House. The KIM Department at CSIR-IICT is acknowledged for providing the Institutional Publication Number IICT/Pubs./2025/009.

Author Contributions RK and SC conceived and designed the study. RK, SP, and SC were involved in performing the experiments and data analysis. YK and PS contributed in performing a part of investigation and data generation. RK and SP wrote the original draft. SC and AK participated in project administration, formal analysis, funding acquisition, reviewing and made the edits to make the final version. SC supervised all the experiments performed in the present study.

Funding This study was initiated under Council of Scientific and Industrial Research (CSIR) Network Project (BSC0115-miND to SC and AK) and later supported by the Indian Council of Medical Research (ICMR) Grant (5/4-5/3/17/Neuro/2022-NCD-1) to SC. RK and SP would like to express their gratitude to CSIR-India for providing their Doctoral Fellowships.

Data Availability Experimental data will be made available on request to corresponding author.

Declarations

Conflict of interest The authors declare that they have no competing interests.

Ethical Approval All animal procedures were approved by the Institutional Animal Ethics Committee, 20/GO/RBi/99/CPCSEA at the Centre for Cellular and Molecular Biology, Hyderabad, India.

Open Access This article is licensed under a Creative Commons Attribution-NonCommercial-NoDerivatives 4.0 International License, which permits any non-commercial use, sharing, distribution and reproduction in any medium or format, as long as you give appropriate credit to the original author(s) and the source, provide a link to the Creative Commons licence, and indicate if you modified the licensed material. You do not have permission under this licence to share adapted material derived from this article or parts of it. The images or other third party material in this article are included in the article's Creative Commons licence, unless indicated otherwise in a credit line to the material. If material is not included in the article's Creative Commons licence and your intended use is not permitted by statutory regulation or exceeds the permitted use, you will need to obtain permission directly from the copyright holder. To view a copy of this licence, visit http://creativecommons.org/licenses/by-nc-nd/4.0/.

References

Akinmoladun AC, Obadaye TS, Olaleye MT, Akindahunsi AA (2021) Prophylaxis with a multicomponent nutraceutical abates transient cerebral ischemia/reperfusion injury. J Food Biochem 45:e13351

Bhanji JP, Delgado MR (2014) The social brain and reward: social information processing in the human striatum. Wiley Interdiscip Rev Cogn Sci 5:61–73

Bhat JA, Kumar M (2022) Neuroprotective effects of theobromine in permanent bilateral common carotid artery occlusion rat model of cerebral hypoperfusion. Metab Brain Dis 37:1787–1801

Bin BD, Kwon KJ, Choi D-H, Shin CY, Lee J, Han S-H, Kim HY (2017) Chronic cerebral hypoperfusion induces post-stroke dementia following acute ischemic stroke in rats. J Neuroinflamm 14:1–12

Bowen KK, Naylor M, Vemuganti R (2006) Prevention of inflammation is a mechanism of preconditioning-induced neuroprotection against focal cerebral ischemia. Neurochem Int 49:127–135

Brancaccio P, Anzilotti S, Cuomo O, Vinciguerra A, Campanile M, Herchuelz A, Amoroso S, Annunziato L, Pignataro G (2022) Preconditioning in hypoxic–ischemic neonate mice triggers Na^+–Ca^{2+} exchanger-dependent neurogenesis. Cell Death Discov 8:318

Burnier L, Boroujerdi A, Fernández JA, Welser-Alves JV, Griffin JH, Milner R (2016) Physiological cerebrovascular remodeling in response to chronic mild hypoxia: a role for activated protein C. Exp Neurol 283:396–403

Burton TM, Madsen TE, Karb R, Furie KL (2024) Importance of sex and gender differences in enrollment and interpretation of stroke clinical trials. J Stroke Cerebrovasc Dis 33(8):107735

Choi B-R, Kim D-H, Bin BD, Kang CH, Moon W-J, Han J-S, Choi D-H, Kwon KJ, Shin CY, Kim B-R (2016) Characterization of white matter injury in a rat model of chronic cerebral hypoperfusion. Stroke 47:542–547

Das T, Soren K, Yerasi M, Kamle A, Kumar A, Chakravarty S (2020) Molecular basis of sex difference in neuroprotection induced by hypoxia preconditioning in zebrafish. Mol Neurobiol 57:5177–5192

de Aguiar RP, Newman-Tancredi A, Prickaerts J, de Oliveira RMW (2021) The 5-HT1A receptor as a serotonergic target for neuroprotection in cerebral ischemia. Prog Neuro-Psychopharmacol Biol Psychiatry 109:110210

Dos Santos EV, de Schirmer BGA, Pereira JM, Cardoso NVS, Malamut C, de Oliveira ML (2023) Applicability of [^{18}F] FDG/PET for investigating rosmarinic acid preconditioning efficacy in a global stroke model in mice. Braz J Pharm Sci 59:e21555

Du Y, Yan C, Wang Y, Xu Y, Cun X, Gao H (2024) The implication and application of brain glymphatic system in multiple diseases. Adv Ther 7:2400088

Erta M, Quintana A, Hidalgo J (2012) Interleukin-6, a major cytokine in the central nervous system. Int J Biol Sci 8:1254

Geng X, Wang Q, Lee H, Huber C, Wills M, Elkin K, Li F, Ji X, Ding Y (2021) Remote ischemic postconditioning vs. physical exercise after stroke: an alternative rehabilitation strategy? Mol Neurobiol 58:3141–3157

Halder SK, Kant R, Milner R (2018) Chronic mild hypoxia promotes profound vascular remodeling in spinal cord blood vessels, preferentially in white matter, via an $\alpha_5\beta_1$ integrin-mediated mechanism. Angiogenesis 21:251–266

Jeong S, Chokkalla AK, Davis CK, Jeong H, Chelluboina B, Arruri V, Kim B, Narman A, Bathula S, Arumugam TV (2024) Circadian-dependent intermittent fasting influences ischemic tolerance and dendritic spine remodeling. Stroke 55:2139–2150

Jing Z, Shi C, Zhu L, Xiang Y, Chen P, Xiong Z, Li W, Ruan Y, Huang L (2015) Chronic cerebral hypoperfusion induces vascular plasticity and hemodynamics but also neuronal degeneration and cognitive impairment. J Cereb Blood Flow Metab 35:1249–1259

Kawata H, Yoshida K, Kawamoto A, Kurioka H, Takase E, Sasaki Y, Hatanaka K, Kobayashi M, Ueyama T, Hashimoto T (2001) Ischemic preconditioning upregulates vascular endothelial growth factor mRNA expression and neovascularization via nuclear translocation of protein kinase C ε in the rat ischemic myocardium. Circ Res 88:696–704

Kelly S, McCulloch J, Horsburgh K (2001) Minimal ischaemic neuronal damage and HSP70 expression in MF1 strain mice following bilateral common carotid artery occlusion. Brain Res 914:185–195

Kim M-S, Kim B-Y, Kim JI, Lee J, Jeon WK (2023) Mumefural improves recognition memory and alters ERK-CREB-BDNF signaling in a mouse model of chronic cerebral hypoperfusion. Nutrients 15:3271

Laforce R Jr, Doyon J (2001) Distinct contribution of the striatum and cerebellum to motor learning. Brain Cogn 45:189–211

Lee D, Tomita Y, Yang L, Negishi K, Kurihara T (2022) Ocular ischemic syndrome and its related experimental models. Int J Mol Sci 23:5249

Lier J, Streit WJ, Bechmann I (2021) Beyond activation: characterizing microglial functional phenotypes. Cells 10:2236

Murry CE, Jennings RB, Reimer KA (1986) Preconditioning with ischemia: a delay of lethal cell injury in ischemic myocardium. Circulation 74:1124–1136

Neumann JT, Thompson JW, Raval AP, Cohan CH, Koronowski KB, Perez-Pinzon MA (2015) Increased BDNF protein expression after ischemic or PKC epsilon preconditioning promotes electrophysiologic changes that lead to neuroprotection. J Cereb Blood Flow Metab 35:121–130

Ojo OB, Amoo ZA, Olaleye MT, Jha SK, Akinmoladun AC (2023) Time and brain region-dependent excitatory neurochemical alterations in bilateral common carotid artery occlusion global ischemia model. Neurochem Res 48:96–116

Patel S, Govindarajan V, Chakravarty S, Dubey N (2024) From blood to brain: exploring the role of fibrinogen in the pathophysiology of depression and other neurological disorders. Int Immunopharmacol 143:113326

Pekny M, Wilhelmsson U, Tatlisumak T, Pekna M (2019) Astrocyte activation and reactive gliosis—a new target in stroke? Neurosci Lett 689:45–55

Radhakrishnan M, Undru A, Patel S, Sharma P, Kumar A, Chakravarty S (2024a) Transcriptomic profiling reveals sex-specific epigenetic dynamics involving kdm6b and H3K27 methylation in cerebral ischemia-induced neurogenesis and recovery. Neuromol Med 26:49

Radhakrishnan M, Vijay V, Supraja Acharya B, Basuthakur P, Patel S, Soren K, Kumar A, Chakravarty S (2024b) Uncovering sex-specific epigenetic regulatory mechanism involving H3k9me2 in neural inflammation, damage, and recovery in the internal carotid artery occlusion mouse model. Neuromol Med 26:3

Shansky RM, Murphy AZ (2021) Considering sex as a biological variable will require a global shift in science culture. Nat Neurosci 24:457–464

Soares LM, Schiavon AP, Milani H, de Oliveira RMW (2013) Cognitive impairment and persistent anxiety-related responses following bilateral common carotid artery occlusion in mice. Behav Brain Res 249:28–37

Stadler J, Schurr H, Doyle D, Garmo L, Srinageshwar B, Spencer MR, Petersen RB, Dunbar GL, Rossignol J (2022) Temporal profile of reactive astrocytes after ischemic stroke in rats. Neuroglia 3:99–111

Tang T, Hu L, Liu Y, Fu X, Li J, Yan F, Cao S, Chen G (2022) Sex-associated differences in neurovascular dysfunction during ischemic stroke. Front Mol Neurosci 15:860959

Ueno K, Samura M, Nakamura T, Tanaka Y, Takeuchi Y, Kawamura D, Takahashi M, Hosoyama T, Morikage N, Hamano K (2016) Increased plasma VEGF levels following ischemic preconditioning are associated with downregulation of miRNA-762 and miR-3072-5p. Sci Rep 6:36758

Varghese SM, Patel S, Nandan A, Jose A, Ghosh S, Sah RK, Menon B, Athira KV, Chakravarty S (2024) Unraveling the role of the blood–brain barrier in the pathophysiology of depression: recent advances and future perspectives. Mol Neurobiol 61(12):1–50

Wahul AB, Joshi PC, Kumar A, Chakravarty S (2018) Transient global cerebral ischemia differentially affects cortex, striatum and hippocampus in bilateral common carotid arterial occlusion (BCCAo) mouse model. J Chem Neuroanat 92:1–15

Wang L, Du Y, Wang K, Xu G, Luo S, He G (2016) Chronic cerebral hypoperfusion induces memory deficits and facilitates Aβ generation in C57BL/6J mice. Exp Neurol 283:353–364

Weinstein JR, Koerner IP, Möller T (2009) Microglia in ischemic brain injury. Future Neurol 5:227–246

Xiao F, Zhang X, Ni P, Yu H, Gao Q, Li M, Huo P, Wei Z, Wang S, Zhang Y (2021) Voltage-dependent potassium channel Kv4.2 alleviates the ischemic stroke impairments through activating neurogenesis. Neurochem Int 150:105155

Yang T, Sun Y, Li Q, Li S, Shi Y, Leak RK, Chen J, Zhang F (2020) Ischemic preconditioning provides long-lasting neuroprotection against ischemic stroke: the role of Nrf2. Exp Neurol 325:113142

Zhao Y, Gong C-X (2015) From chronic cerebral hypoperfusion to Alzheimer-like brain pathology and neurodegeneration. Cell Mol Neurobiol 35:101–110

Publisher's Note Springer Nature remains neutral with regard to jurisdictional claims in published maps and institutional affiliations.